



Comparison of surface-engineered superparamagnetic nanosorbents with low-cost adsorbents of cellulose, zeolites and biochar for the removal of organic and inorganic pollutants: a review

Dhanya Vishnu¹ · Balaji Dhandapani¹ · Gopinath Kannappan Panchamoorthy¹ · Dai-Viet N. Vo² · Shankar Ram Ramakrishnan¹

Received: 8 January 2021 / Accepted: 5 February 2021 / Published online: 10 March 2021
© The Author(s), under exclusive licence to Springer Nature Switzerland AG 2021

Abstract

Industrialization and human activities have led to pollution of ecosystems by metals and dyes, calling for advanced remediation methods. For instance, removal of water pollutants has been recently done using low-cost adsorbents. Here we review adsorbents based on cellulose, zeolites, biochar and nanomaterials. Hybridized nanosorbents show adsorption capacities up to five times higher than single materials, due to the combination of functions such as carboxyl, amino, thiol, hydroxyl, vinyl, metals and phenolics. Integrating metals having high magnetization and superparamagnetic properties improves reusability up to 10 cycles with minimal loss of pollutant removal efficiency.

Keywords Adsorption · Hybridized nanosorbent · Pollutants · Remediation

Abbreviations

BET	Brunauer–Emmett–Teller
CTAB	Cetyl trimethyl ammonium bromide
EDS	Energy dispersive spectroscopy
FESEM	Field emission scanning electron microscope
FTIR	Fourier transform infrared spectroscopy
HRTEM	High-resolution transmission electron microscope
NMR	Nuclear magnetic resonance
SEM	Scanning electron microscope
TEM	Transmission electron microscope
TGA	Thermogravimetric analysis
XPS	X-ray photoelectron spectroscopy
XRD	X-ray Diffraction

Introduction

There is interest in the creation of novel magnetic particles and their substantial use in the treatment of wastewater effluents. The synthesis and the application of these magnetic particles are considered to be fast, relatively cost comparable and eco-friendlier in the discharge of toxic contaminants when compared to the other conventional technologies. The conventional treatment methodology includes both physical and chemical approaches that remove the expensive and toxic contaminants causing the major risk to the environment (Xue et al. 2017). Although these traditional methods like filtration, flocculation, coagulation, and mechanical separation are used, the increase in the level of the contaminants provokes a need for some advanced technologies with improved efficiency (Crini and Lichtfouse 2019). The major lead in the usage of these magnetic particles is due to their unique superparamagnetic feature, enhanced adsorption capacities and specifically high surface area to the volume ratio (Soares et al. 2020). Based on the crystalline structure, numerous metallic particles are synthesized such as silver nanoparticles, gold nanoparticles (Perera et al. 2020), zinc oxide nanoparticles, copper oxide nanoparticles and ferrite nanoparticles (Vishnu et al. 2020). These nanoparticles with the size of 1–100 nm could be formulated by both top-down and bottom-up approaches (Prakash Sharma et al. 2018). The approach mainly concentrates on the design and non-design

✉ Balaji Dhandapani
balajid@ssn.edu.in; dbalajii@yahoo.com

¹ Department of Chemical Engineering, Sri Sivasubramaniya Nadar College of Engineering, Chennai 603 110, India

² Center of Excellence for Green Energy and Environmental Nanomaterials (CE@GrEEN), Nguyen Tat Thanh University, Ho Chi Minh City 755414, Vietnam

criteria, and they are highly evaluated on the processing of material, ease of manufacturing, end product usage and their risk assessment (Cai 2020). Table 1 illustrates the synthesis of nanoparticles with advantages and disadvantages. The small size and high surface area of these particles entrap pollutants with a high efficient capacity when they are contacted with the contaminated water (Prakash Sharma et al. 2018).

The numerous contaminants in the contaminated sites are listed as hazardous metallic contaminants, and organic pollutants such as pharma products, pesticides, and dyes. These pollutants remain in the aquatic system and deteriorate the health of both aquatic organisms and the social human communities of the ecosystem (Abdelbasir and Shalan 2019). Agriculture practice is also studied as one of the prominent causes in the release of contaminants to the ecosystem in the form of utilizing toxic pesticides and fertilizers for the enhanced productivity of crops (Makvandi et al. 2020). The numerous activities such as aquaculture using toxic pathogens, silviculture, hazardous chemical substances and various heavy metals could contaminate the quality of groundwater on the consecutive accumulation of toxic contaminants in the environment (Ahmad et al. 2020).

Water treatment is considered as the most necessary technology, as the cost of treatment strategy is the prominent concern among the overall treatment technology. There are different metallic contaminants such as Pb, Ni, Cu, Co, Cd, Cr, Hg and Zn released into the ecosystem as the industrial pollutants from electroplating, leather tanneries and mineral processing areas (Malik et al. 2019). Chemical wastes are figured as a major threat and cause deleterious effects on the aquatic environment. The treatment process and recovery of water from them are challenging outcome and complex processes. Dyes are figured as one of the main chemical wastes, and their primary usage is from the textile industries.

They are also widely used in the other industries of wool, leather, paper and silk. The complex aromatic structure in dye molecules is the main problem of degradation (Kasiri and Safapour 2014). Since they possess stable and thermal resistance against degradation, they prevail in water for a long duration and cause much severe threat to the aquatic environment (Chowdhary et al. 2018).

Adsorption is predominantly considered among the other treatment methodologies such as ion exchange, reverse osmosis, phytoextraction, electrodialysis, etc. Adsorption could reduce the operational cost and high energy consumption on its application in large scale. The widely used adsorbents from several fruits and agricultural waste of low cost are the added advantage of this process (Vicente-Martinez et al. 2020).

The two types of sorption strategies are physisorption and chemical adsorption. Physisorption occurs through forces between the hydrogen bond of the particles, Vander Waal's forces, etc. Chemisorption occurs when the pollutants are attracted to the adsorbent through a chemical bond (Crini and Lichtfouse 2019). Magnetic particles integrated with the numerous enzymes and metallic sites are used to produce numerous bio-valuable end-products. Because of their vital and unique characteristic features, these particles are preferred as the adsorbing materials in the discharge of metals and toxic dye contaminants (Vishnu et al. 2019, 2017).

Exhaustive analysis in the present studies reveals that the specific entities integrated upon the surface of the sorbent predominantly enhance the metallic binding and in degrading the complex aromatic groups. The hybridized metallic magnetic particles integrated with the natural adsorbents acts as the promising alternative sorbents in the removal of both metal and dye molecules. Hereby, the present study justifies the current exploration over the numerous magnetic

Table 1 Various approaches of nanoparticle synthesis with merits and demerits

Top-down approach	Bottom-up approach	Advantages of top-down and bottom-up approach	Nanoparticle synthesis
Mechanical milling	Vapour deposition	Bio reductions	Disadvantages—Top-down and bottom-up approach
Chemical etching	Laser pyrolysis	Low energy consumptions and low cost	Expensive
Thermal ablation	Spray pyrolysis	Eco-friendlier method that eliminates the discharge of noxious secondary products to the ecosystem	Release of toxic by-products
Sputtering	Sol-gel process	The polyphenolic constituents act as reducing and capping agents	High temperature and pressure conditions
Explosion processes	Aerosol process	High temperature and pressure are not necessary	
	Spinning		
	Atomic/molecular condensation		
	Chemical vapour deposition		
	Molecular beam epitaxy		
	Physical vapour deposition		
	Synthesis of nanoparticles using		
	Bioreduction—		
	Precipitation		
	Microbial sources (Bacteria, fungi and yeast)		
	Plant materials (Leaves, stems, seeds, flowers)		
	DNA, cell lines, membranes		

sorbents coated with specific substances to enhance the surface area that has been induced with numerous functional entities to enhance the remediation process.

Sources of pollutants

Dyes are the organic pollutants released from numerous industries, get mixed with the natural resources and could cause various deleterious effects on the organisms in the aquatic environment. Appropriately, ten thousand numerous dyes were released by the industries and around 0.7 million tonnes were produced in global markets. Based on the various sources, dyes are formulated under natural and synthetic dyes. Natural dyes are obtained from some plant sources, whereas the synthetic dyes are derived from organic and inorganic constituents. Based on the charges, dyes are categorized into anionic, cationic and non-ionic dyes (Ngulube et al. 2017).

Acidic dyes include acid yellow, acid violet 90, acid blue 193 that are used in the fabrication of microfiber nylon. Basic dyes include Basic green 4 that is used in the Acrilan products. Direct dyes include Direct yellow 12 and Direct yellow 27 that are used in the synthesis of cotton stuff (Nidheesh et al. 2018). Dispersed and the reactive dyes include pyrazole disperse dyes, Levafix red, blue and yellow CA that are mainly used to fabricate wool, nylon and cotton fabrics (Xiao et al. 2019b). Researchers have studied and categorized dyes as acidic, reactive, basic, vat, direct and azo dyes. The below schematic representation (Fig. 1) gives the detail about the various classification of dyes and the adsorbents used in the discharge of dye contaminants (Azari

et al. 2020). Figure 2 describes the adverse effects of toxic metal and dye molecules.

Industrialization and urbanization result in the sequential accumulation of metal contaminants such as Cu, Ni, As, Pb, Zn, Fe and Cd in the water reservoirs. These heavy metals show their toxic behaviour beyond certain permissible limits when consumed by the other organisms and human beings present in the environment (Xin et al. 2012). Table 2 represents the permissible limit of each metal and their toxic effects on continuous intake.

Treatment strategies used in the discharge of dyes and metal pollutants

Physical, chemical and biological treatment methodologies are adopted in the assessment of noxious dyes and metallic pollutant discharge. The physio-chemical method includes coagulation, flocculation, ozonation and the biological treatment is mainly necessary for the removal of noxious metallic contaminants, nitrogen, phosphorous and organic constituents. Figure 3 explains the various physical, chemical and biological treatment processes. The disadvantages of these process are listed as the excessive formation of sludge, consumption of huge space, the complex non-bio-degradable nature of the dyes, the long time needed for the treatment process. This leads to the treatment of industrial effluents to be categorized under three systematic processes of primary, secondary and tertiary treatments (Ghosh et al. 2016).

The primary treatment process involves the screening of the effluents with sedimentation and flocculation to remove the unwanted suspended particles. Primary treatment reduces the vital parameters of suspended particles, biological oxygen demand, chemical oxygen demand,

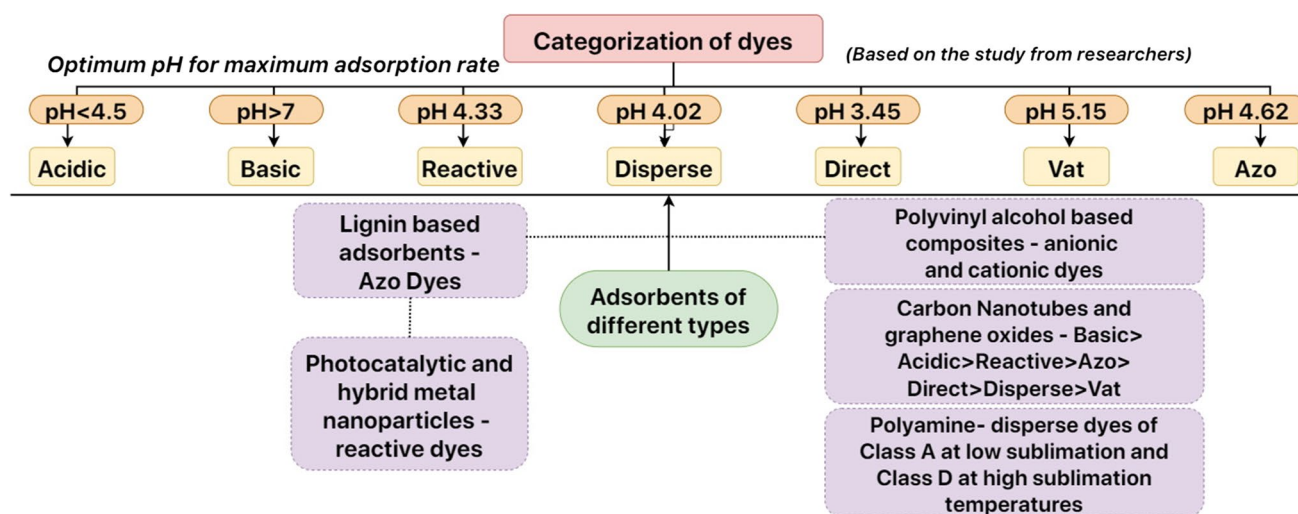


Fig. 1 Dye categorization and their effect on different pH and adsorbent types

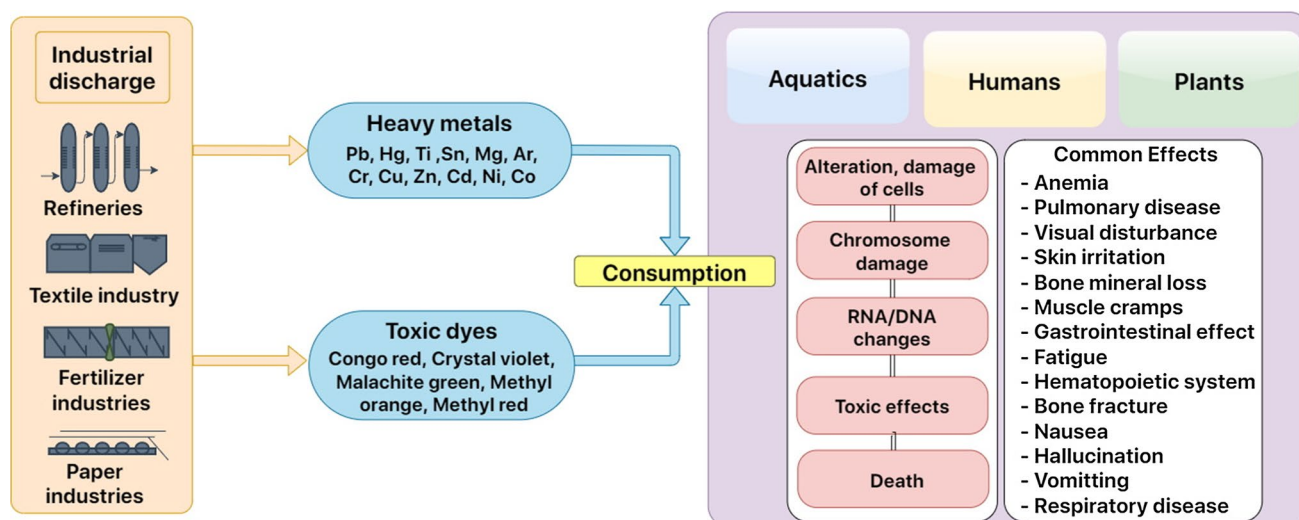


Fig. 2 Accumulation of heavy metals and dyes in the aquatic system and adverse effect of the floral ecological communities in the ecosystem

Table 2 Heavy metals with permissible limits and deleterious effects

Heavy metal	Permissible limits (mg/L)	Deleterious effects	References
Arsenic	0.05	Several types of cancer and problems in the circulatory system	Bashir et al. (2019)
Cadmium	0.005	Kidney associated health issues	Bashir et al. (2019)
Chromium	0.1	Dermatitis associated health issues	Paul (2017)
Copper	1.3	Kidney and liver-related associated with gastrointestinal health effects	Paul (2017)
Lead	0.05	Physically associated with mental stress that enhances the kidney-related effects with the outcome of high blood pressure	Bashir et al. (2019)
Mercury	0.002	Affects the kidney	Paul (2017)
Selenium	0.05	Causes hair loss and blood circulated issues	Malik et al. (2019)
Zinc	0.15	Skin irritation	Bashir et al. (2019)

bacteria and other organic matters. Figure 4 represents the reduction of the above parameters after the primary treatment strategy. The demerits of the primary treatment strategy are the sludge disposal after the treatment process (R Ananthashankar 2013).

The secondary treatment process is sequestered in the presence of various microbial sources subjected to aerobic or anaerobic conditions. In this method, BOD is reduced with the enhanced removal efficiency of 99% with 15–25% phosphorous removal. Sludge generation is controlled by the anaerobic treatment, and the disadvantage of this system is the contamination of microbial sources and the need for the laborious space to set up the equipment (Abd El-Rahim et al. 2017).

The tertiary treatment process includes ion exchange, reverse osmosis and the electro dialysis techniques (Ghasemipanh 2013). The membrane separation technique separates the contaminants from the water. The greatest disadvantage

of this method was membrane fouling (Marcucci et al. 2002). Among several techniques, adsorption is considered as the prominent cost-effective treatment strategy used to reduce both organic and inorganic contaminants.

Classification of various adsorbents

Adsorbents, based on the surface structural characteristics and chemical nature, are broadly classified as natural and synthetic adsorbents. Natural adsorbent materials like sawdust and wood derivatives are chemically modified by acids and alkali, have been used to discharge the metallic and organic pollutants. Synthetic adsorbents such as polymeric resins and aluminosilicates, adsorbents prepared from the agricultural residues and the microbial sources of bacteria and fungi are incorporated into chitosan materials and act as the sorbents to remove the organic and inorganic

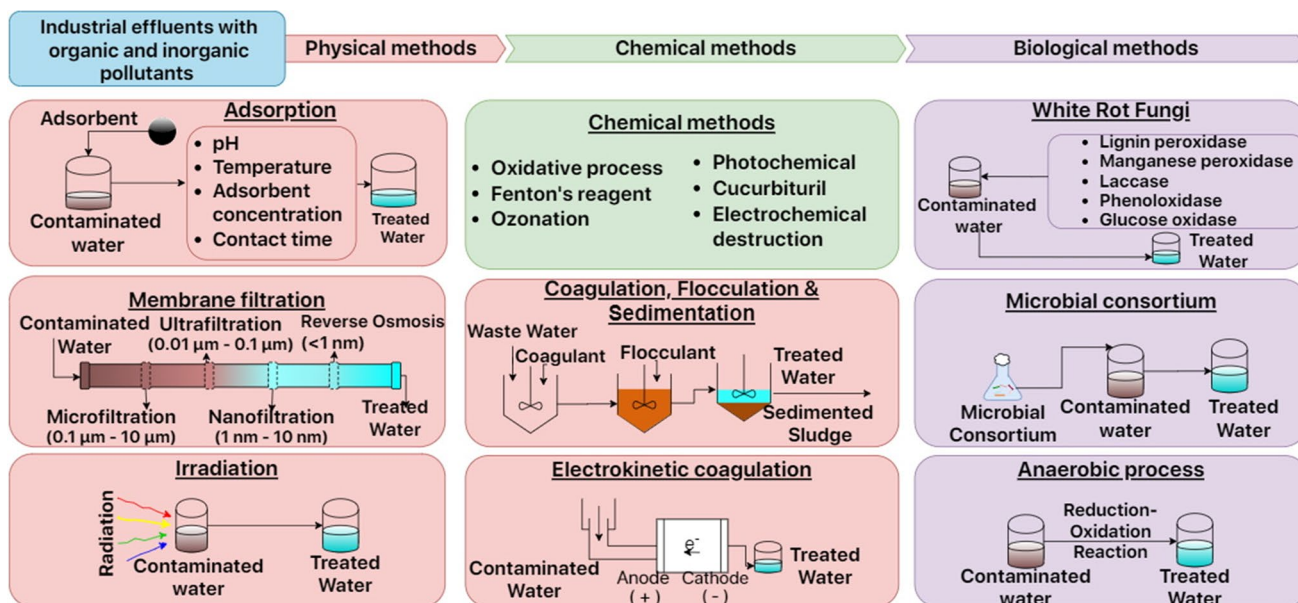
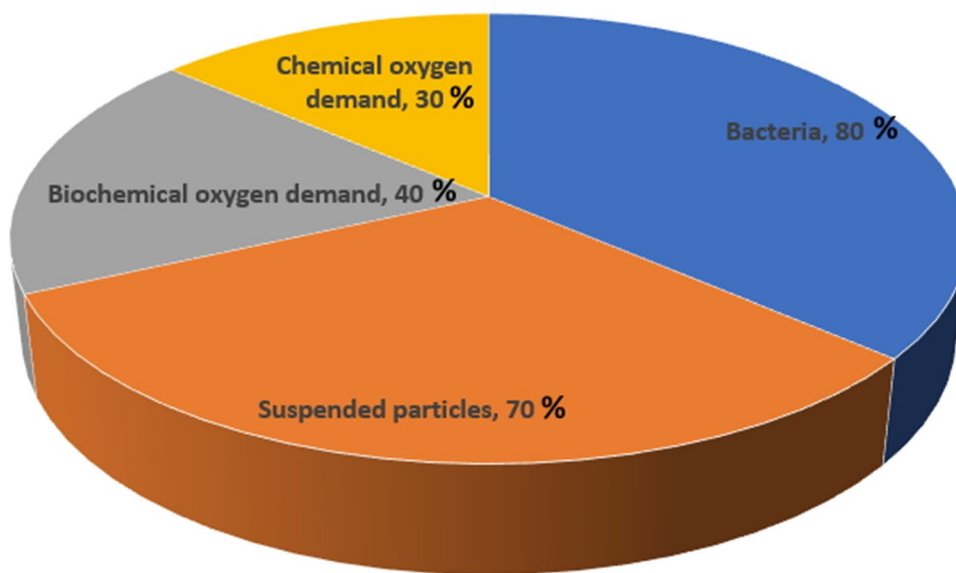


Fig. 3 Physical, chemical and biological treatment methods used in the removal of dyes and metallic contaminants

Fig. 4 Percentage reduction of various pollutants after primary treatment technology



contaminants from the ecological communities (Pavithra et al. 2019). Figure 5 illustrates the classification of various adsorbent materials.

The adsorbent was categorized as conventional and non-conventional adsorbents. Activated carbon is prominently used as efficient adsorbents in many industries. It enhances the adsorption rate with the adsorption capacity of the overall phenomena. The demerits are expensive, non-selective phenomena, and it cannot be reused and regenerated. It requires a huge consumption of energy (Crini et al. 2019a). Table 3 gives a detailed description of the conventional and non-conventional adsorbents that are formulated to discharge

the numerous organic and inorganic pollutants from the waste effluents (Crini et al. 2019a).

Adsorption mechanism

The mechanism of solute that gets adsorbed into the adsorbent surface constitutes a pioneering role in the removal rate of contaminants. The adsorption capacity mostly differs on the selectivity of the material as an adsorbent, laborious cost, various operational parametric constituents of pH, contact time, temperature, the concentration of the adsorbent and the

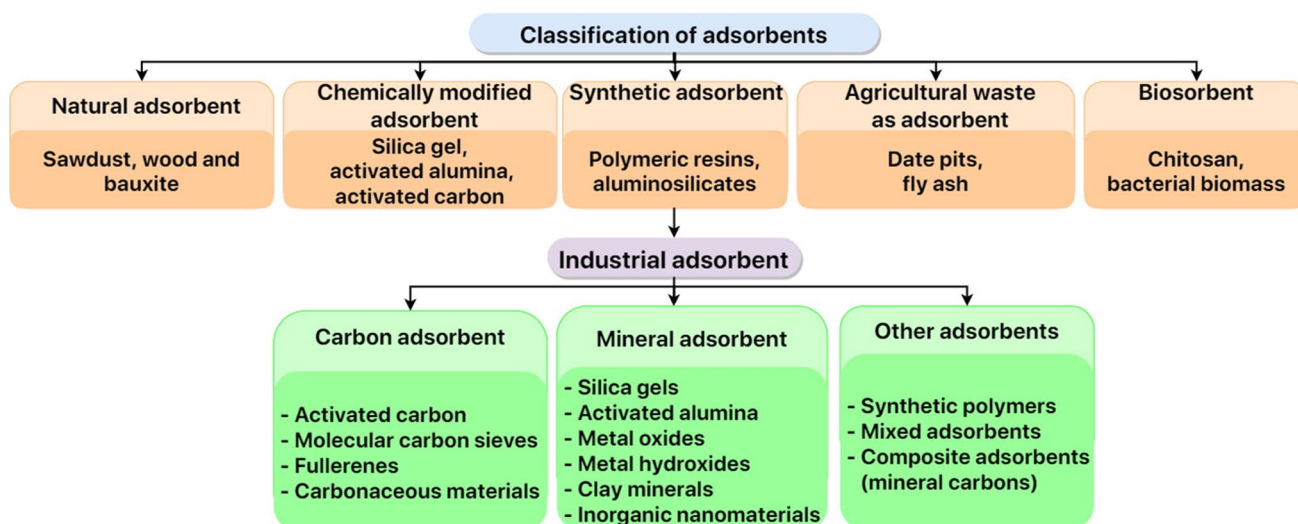


Fig. 5 Classification of adsorbents and the various industrial low-cost adsorbents used in the removal of dyes and metal pollutants

Table 3 Classification of conventional and non-conventional adsorbents

Conventional	Commercial Activated carbon Wood Peat Coconut shells Coals Anthracite Bituminous lignite		Inorganic materials Activated alumina Silica gel Zeolites Molecular sieves		Ion-exchange resins Polymeric organic resins Non-porous resins Porous resins crosslinked with each other	
Non-Conventional adsorbent	Natural Clays, Siliceous materials, Inorganic materials	Agricultural residues Bark, Sawdust, Solid waste	Industrial products Fly ash, Sludge, Metal hydroxide sludge, Red mud	Activated carbon from solid residues Agricultural solid waste, Industrial by-products	Biosorbents Biomass from microbial sources, Peat, Chitosan, polysaccharides	Miscellaneous adsorbents Cotton waste products, Calixarenes, Hydrogels

metal contaminants. Adsorption phenomena are explained in the overall three steps (Sherlala et al. 2018; Das 2010).

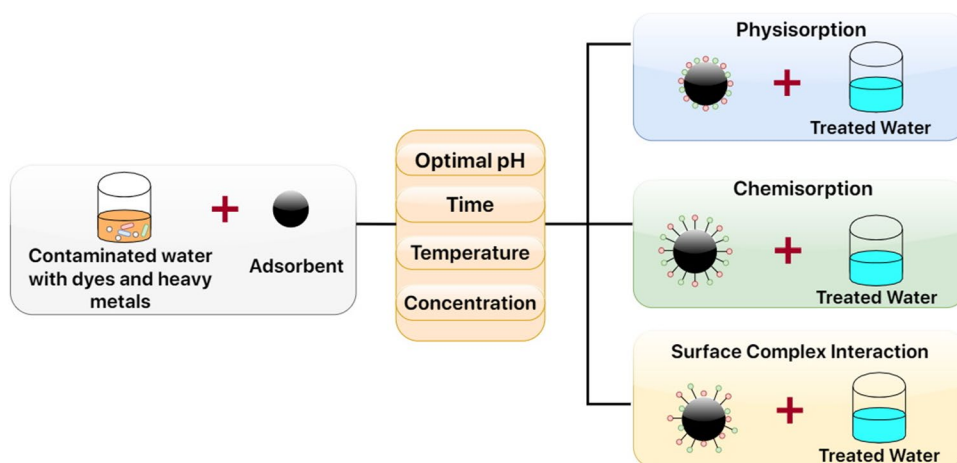
- Film diffusion—Mass transfer of solute particles that gets the film to the exterior surface of the adsorbing material.
- Solid surface diffusion—Adsorbate gets diffused inside the pores of the adsorbent.
- Adsorbate gets interacted with the adsorbent through physical forces or chemical binding between them.

Based on the interaction type, adsorption is majorly categorized as physisorption and chemisorption. Physisorption occurs through electrostatic surface interactions, hydrogen bonds and van der Waals force attraction

between the adsorbing material and adsorbate molecules. Chemisorption is based on hydrophobic, covalent and complex interactions between the adsorbing material and solute molecules (Fig. 6) (Wan Ngah et al. 2011).

The kinetics and the isotherm models help to explore the rate-determining mechanism of the adsorption process. Pseudo-first-order determines the homogeneous adsorption and pseudo-second-order kinetics model describes the heterogeneous adsorption system (Largitte and Pasquier 2016). Elovich evaluates the complex system of the adsorption process and intraparticle diffusion system determines the diffusion process of adsorbate in the adsorbent (Wang and Guo 2020).

Fig. 6 Mechanism of adsorption and optimal conditions used in the discharge of dyes and metal contaminants



Adsorption isotherm models are examined to evaluate the interactive mechanism between the adsorbate and adsorbent molecules. Based on the equilibrium data and adsorbent characteristics, several isotherm models are predicted and categorized under one parameter isotherm models (Henry), two-parameter isotherm models, three-parameter isotherm models, four-parameter isotherm models and five-parameter isotherm model (Ayawei et al. 2017). The two-parameter models are listed as Langmuir, Freundlich, Dubinin–Radushkevich, Temkin, Flory–Huggins, Hills, Halsey and Jovanovich (Al-Ghouti and Razavi 2020). The three-parameter isotherm models are Langmuir–Freundlich, Redlich–Peterson, Sips, Khan and Toth isotherm model (Foo and Hameed 2010). The four-parameter isotherm models are Fritz–Schlunder, Baudu, Weber–Van Vliet and Marczewski–Jaroniec and the Fritz Schlunder describes the five-parameter isotherm model (Al-Ghouti and Da’ana 2020). Error analysis is required to evaluate the best-fitted isotherm model with the experimental fit (Table 4) and some of the methods are listed in Table 4 (Simsek and Beker 2014).

Cellulose as an adsorbing material in the discharge of pollutants:

Cellulose is preferred as the potent adsorbing material in the discharge of dyes and heavy metals since it has the unique characteristics of renewable, biodegradable, less toxic and highly available nature (Badruddoza et al. 2011). The surface of the cellulose is modified with oxidation, halogenation, sulfonation, esterification and etherification to enhance the adsorption capacity of these dye contaminants. The acid hydrolysed cellulose obtained from oil palm acts as a potent adsorbing material in the discharge of methylene blue dye from the aqueous solution. The crystal and porous nature of cellulose molecules with an enhanced surface area of $5.64 \text{ m}^2 \text{ g}^{-1}$ and unmodified physiological feature upon acid hydrolysis provoke to be a potent adsorbent in the discharge of methylene blue effluent of about 51.81 mg g^{-1} (Hussin et al. 2016).

The surface modification of cellulose enhances the adsorption capacity of 12.85 mg g^{-1} due to the change in the

Table 4 Numerous error analysis methods and their description

Methods	Equation	Description
HYBRID—The hybrid fractional error function	$\frac{100}{n-p} \sum_{i=1}^p \left[\frac{(Q_{\text{exp}} - Q_{\text{cal}})^2}{Q_{\text{exp}}} \right]_i$	Determined at low concentrations. n determines the data points and p represents the isotherm parameter. Q_{exp} and Q_{cal} are the experimental and the calculated values, respectively (Porter et al. 1999)
MPSD -Marquardt’s percent standard deviation	$100 \left[\sqrt{\frac{1}{n-p} \sum_{i=1}^p \left[\frac{(Q_{\text{exp}} - Q_{\text{cal}})^2}{Q_{\text{exp}}} \right]_i} \right]$	To evaluate the degrees of freedom in the process (Simsek and Beker 2014)
EABS—The sum of the absolute errors	$\sum_{i=1}^p (Q_{\text{exp}} - Q_{\text{cal}})_i$	To determine the best fit with an increase in the magnitude errors (Allen et al. 2004)
ARE—The average relative error	$\frac{100}{p} \sum_{i=1}^p \left[\frac{(Q_{\text{exp}} - Q_{\text{cal}})}{Q_{\text{exp}}} \right]_i$	It diminishes the fractional error distribution for the wide concentration range (Demirbas et al. 2008)
ERRSQ—The sum of the squares of the errors	$\sum_{i=1}^p (Q_{\text{exp}} - Q_{\text{cal}})_i^2$	The error gets increased with enhanced concentration (Allen et al. 2004)

morphological features of pore size (enhanced from 2.04 to 9.47 m²g⁻¹) after modification and charge of the compounds covered on the exterior surface. Another study reveals that the successful impregnation of cellulose from oil palm in the glass plate shows the enhanced removal efficiency of methylene blue dyes. The surface area after adsorption of dye depletes to 8.32 m²g⁻¹ that proves the successful incorporation of dyes with cellulose compounds (Tan et al. 2018).

Modified cellulose obtained from the groundnut shell acts as an effective adsorbing material of crystal violet dye with the adsorbent capacity of 79 mgg⁻¹ due to their increased surface area upon chemical modification (Zango and Shehu Imam 2018). Chemically modified cellulose adsorbent was intended more on the discharge of methylene blue dyes with the surface area of 12.55 m²g⁻¹, 30 m²g⁻¹, 36.92 m²g⁻¹ and the adsorbent capacity of 80.1 mgg⁻¹, 101.01 mgg⁻¹ and 142.86 mgg⁻¹. (Wei et al. 2017, 2018; Sun et al. 2016). Cellulose was altered with the ionic liquid (4-methylimidazole) to the microsphere network structure using the sol-gel strategy that used to remove the noxious acid orange 7 dye molecules with the adsorption capacity of 279.45 mgg⁻¹.

The electrostatic interaction with the hydrogen bonding and pi-pi interaction provokes the adsorption of methyl orange dye molecules by the altered microporous cellulose engineered acetate entity embedded on polyurethane sheets amphoteric molecules in them (Iqhrammullah et al. 2020). However, more studies have to be done on the removal of anionic, cationic and other azo dye compounds. Congo red dyes are removed with the maximum adsorption capacity of 304 mgg⁻¹ (Hu et al. 2014).

Cellulose upon surface modified with the polyamide molecules has shown the enhanced adsorption capacity of the orange II dyes, with the increase in the abundant active sites. The propagated three-dimensional structure provokes the strong electrostatic and hydrogen bonding between the surface layered amino terminated polyamide groups and the sulphide group of the complex dye molecules and enhances the adsorption capacity from 13.5 mgg⁻¹ to 1157.9 mgg⁻¹ (Huang et al. 2020). Table 5 describes the characteristics and mechanism of the reaction system of methylene blue and other azo dye compounds, whereas more studies have to be done on the removal of anionic, cationic and other azo dye compounds.

The properties of functional entities, structure, enhanced mechanical, thermal, structural and chemical stability, contact area and adsorbent selectivity could decide the removal efficiency of the heavy metals by any adsorbents (Cao et al. 2019). Though cellulose molecule possesses high mechanical strength and chemical structure for being as a potent adsorbent, the insufficient binding sites lead to the surface modification of cellulose molecules with the specific functional entities. The combination of amino terminated polyamide groups and the hydroxyl entity present in the surface

of three-dimensional structure provokes the strong electrostatic and hydrogen bonding with the copper metal ions with the maximum adsorption capacity of 137.48 mgg⁻¹ compared with the normal cellulose molecule (47.02 mgg⁻¹) (Kong et al. 2020).

The different functional entities of hydroxyl (-OH), thiol (-SH), carboxyl (-COOH), carboxamide (-CONH), amino group (-NH₂) differ in the mechanistic removal of pollutants. The binding between the functional group of graphene with amino, hydroxyl and carboxyl group results in a stronger interaction with lead than copper, whereas the cellulose moiety with carboxamide produces a similar trend in the adsorption of both copper and lead (Kong et al. 2020).

Hydrogels act as the potent adsorbing material in the discharge of copper ion from the aqueous solution. When cellulose material was grafted with styrene molecule, it enhances the adsorption of hexavalent chromium ions from the aqueous solution (Hao et al. 2018). The halogenated cellulose adsorbent with the pyridone diacid removes cobalt and lead ions with the adsorption capacity of 122.7 mgg⁻¹ and 177.75 mgg⁻¹ (Sun et al. 2017). The studies reveal that the chemically modified cellulose molecule acts as the efficient adsorbent in the discharge of metal ions owing to their enhanced surface area and pore volume ratio (El-Naggar et al. 2018; Cao et al. 2017; Tang et al. 2013; Vijayalakshmi et al. 2017). Table 6 represents the modified cellulose acts as the adsorbing material in the discharge of various metal ions.

Zeolites as the adsorbing material in the discharge of pollutants

Natural zeolites could act as the potent cost-effective adsorbing material in discharging the cationic dye pollutants from the contaminated sites. Ammonium is the most prevailing contaminant that causes a severe threat to the aquatic organisms present in the environment. (Ivanković and Hrenović 2010; Ivanković and Hrenović 2010). The removal efficiency correlates with the concentration of the surfactant present in the exterior surface of the zeolite. Many types of research have studied with zeolite as the potent adsorbent and it possesses 68 different structural characteristics (Goyal et al. 2016). Natural zeolites when treated or modified into the low-cost adsorbents proved to be an efficient adsorbent in discharging the toxic dye pollutants owing to their exchange molecules at the extensive surface of the material. Adsorbent gets attached to the exterior surface of the sorbent via physical attraction such as polar nature, hydrogen interaction, dipole attractive forces, Vander Waal's interaction (Kausar et al. 2018).

Adsorption mainly depends on numerous unified feature of size, structural feature, molecular mass and concentration of the solution. Sepiolite, a clay sample acts as the potent adsorbent material in the removal of reactive azo dye molecules.

Table 5 The cellulose used in the removal of noxious dyes

Surface modified cellulose adsorbent	Dye molecules	Adsorption capacity mg/g	Morphological analytic features	Mechanism	References
Modified cellulose aerogels impregnated with graphene oxide	Methylene blue	2630	The network and three-dimensional porous structure were examined through a scanning electron microscope (SEM). Thermogravimetric analysis (TGA) at 347 °C reveals the strong interaction between the graphene and cellulose aerogels. The functional entities and further interactions are studied using Fourier transform infrared spectroscopy (FTIR) and X-ray photoelectron spectroscopy (XPS)	Pseudo-second-order kinetics model and the reaction was dominated by the strong electrostatic interaction between the molecules	Wei et al. (2017)
Modified cellulose on Polydopamine aerogels	Methylene blue	153.4	The network and sheet pattern was examined through SEM. The surface area (36.92 m ² /g) was studied by Brunauer–Emmett–Teller (BET) and the functional entities of the aerogels are studied through FTIR	Pseudo-second-order kinetics model and the Langmuir isotherm model was determined. The reaction was dominated by the strong electrostatic interaction and pi-pi interactions between the aromatic structural molecules	Wei et al. (2018)
Cellulose modified with pyridone	Methylene blue	142.86	The rough crystalline structure was examined through SEM and nuclear magnetic resonance (NMR), the coated functional entities are examined through FTIR and TGA was observed at 400 °C	Pseudo-second-order kinetics model and the Langmuir isotherm model was determined. The reaction was dominated by strong electrostatic interaction and hydrogen bonding	Sun et al. (2016)
Cellulose modified with N, N-dimethyl dodecyl amine	Congo red	303.34	The porous and coarse nature was examined through SEM. FTIR and X-ray diffraction (XRD) confirms the functional entities of the coated molecules	From the zero point charge (7.68) evaluation the reaction was dominated through electrostatic interactions between the molecules	Hu et al. (2014)
Cellulose altered with acetate group on polyurethane sheet	Methyl orange	279.45	The porous microsphere nature was analysed through FTIR, SEM and	The system follows the Pseudo second-order model and Freundlich isotherm model. The reaction was dominated through electrostatic interaction with pi-pi interaction and hydrogen bonding	Iqhrammullah et al. (2020)
Modified cellulose with the amino grouped polyamide molecules	Acid black, Methylene blue	1157.9, 13.5	The crystal nature and functional entities of the compound are studied by FTIR, NMR, TGA, SEM, XPS and zeta potential	The Phenomena follows pseudo-second-order reaction and Langmuir isotherm model. The reaction was dominated through electrostatic interaction and hydrogen bonding	Huang et al. (2020)

The fabricated zeolites showed potent improvement owing to their silica-alumina content of the particle which provides the enhanced surface area of $190.2 \text{ m}^2\text{g}^{-1}$, that increases overall sorption phenomena (Arefi Pour et al. 2016). Though the hydrophilic entities on the zeolite surface retard the adsorption of non-ionic groups, surface modified treatment via acids and alkali enhances the adsorption through crosslinking and ion exchange mechanism (Zhou et al. 2019).

The mechanism behind the dye removal with the hydroxyl groups layered upon the zeolite surface has been depicted in the below-given Eq. (1). The surface area enhances the specific induction of entities upon acid and alkali treatment, prominently enhances the overall adsorption phenomena appropriately (Hernández-Montoya et al. 2013).

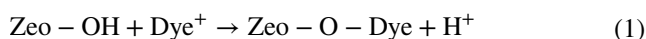


Table 7 represents the zeolite as the adsorbing material in the discharge of numerous toxic dye contaminants. Heavy metal removal with the zeolites depends on the type of metal ion and their binding affinity with the zeolites. A Bulgarian natural zeolite when chemically modified with the acid and alkali molecules such as HCl, NaCl, NaOH and CH_3COONa , they act as the enhanced adsorbent in the removal of numerous metal ions like copper (6.3 mgg^{-1}), cadmium (5.8 mgg^{-1}), nickel (3.2 mgg^{-1}) and zinc (4.0 mgg^{-1}) (Wang and Peng 2010). The mechanism behind the adsorption of metals with Zeolites has been observed in the two different equations. The possible interaction between the metal contaminants with the hydroxyl group contaminants was ascribed in Eq. (2) and the ion exchange phenomena with the negative charges balancing within the structural feature of the zeolites have been described in the Eq. (3) (Hernández-Montoya et al. 2013).

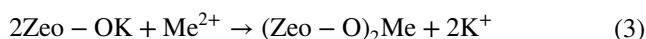
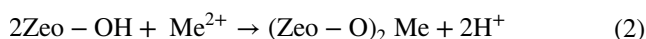


Table 8 represents the zeolites as the adsorbing material in the removal of various heavy metal contaminants. The reaction mechanistic procedure pioneered to be ion exchangeable reaction where surface entities of the zeolite molecules adsorb cation/anions (Zhou et al. 2019). The selective and competitive behaviour in multiparticle adsorption phenomena attracts researchers to use as a potent adsorbent, despite limitations (Zhou et al., 2019).

Biochar as the adsorbing material in the discharge of pollutants.

Biochar made from various biomass composites of crop waste constituents, food and agricultural waste

components, animal wastes and sludge composites acts as the robust adsorbent in removing various pollutants. Metals affiliated with specific entities such as hydroxyl, carboxyl and alcoholic moieties that were extensively distributed in surface of biochar (Chao et al. 2018). The morphological and physiological traits of the biochar are based on the modified constituents of carbon and grey obtained at various pyrolysis temperature and choice of the base material used for the fabrication of biochar. The low-cost effective biochar adsorbent has emerged researchers to use it in the discharge of various toxic dye molecules (Dai et al. 2019).

Three types of biochar derived from pine wood, pig manure and cardboard have proved to be the robust adsorbent in the removal of methylene dye molecules due to the presence of high ash content in the biochar molecule (Lonappan et al. 2016). The biochar obtained from the tree *Gliricidia sepium* produced at the three different pyrolysis temperature of $300 \text{ }^\circ\text{C}$, $500 \text{ }^\circ\text{C}$ and $700 \text{ }^\circ\text{C}$ shows the promising result in the removal of crystal violet dye with an enhanced adsorption capacity of 125.5 mgg^{-1} . The biochar prepared at various temperature shows the different range of carbon, hydrogen and nitrogen content, where the high surface area of $808 \text{ m}^2\text{g}^{-1}$ and pore volume ($0.89 \text{ cm}^3\text{g}^{-1}$) was obtained at a higher temperature.

The morphological traits of pore size, volume, extensive surface moieties produce physical interaction of Van der Waals forces, pi-pi electron interchanging mechanism between the adsorbent and pollutants. Chemical interactions between the negative moieties on the surface of the pollutants and dye molecule. The enhanced performance is attained via a combination of physicochemical interaction between the sorbent and dye (Wathukarage et al. 2019). The biochar obtained from pecan nutshell shows excellent behaviour in the removal of Direct red 4BS with the adsorption capacity of 59.77 mgg^{-1} from the aqueous solution.

Physical traits of an area, surface area ($29.18 \text{ m}^2\text{g}^{-1}$) and pore volume (0.058) promote physical interaction between the surface of biochar and pollutants through exterior pore diffusion, whereas the extensive carbonyl, carboxylate and hydroxyl moieties promote electrostatically and pi to pi interaction between them. It was inferred from studies that Direct red, methylene blue and rhodamine interact with hydroxyl, whereas acetyl orange binds with the carboxyl group of biochar molecule (Chen et al. 2019). The biochar obtained from the *Caulerpa scalpelliformis* shows excellent behaviour in the discharge of Remazol Brilliant blue R ($0.2279 \text{ mmolg}^{-1}$), Remazol Brilliant orange 3R ($0.2311 \text{ mmolg}^{-1}$), violet 5R ($0.2171 \text{ mmolg}^{-1}$), black B ($0.1781 \text{ mmolg}^{-1}$) (Gokulan et al. 2019) and basic yellow dye (27

Table 6 Cellulose materials used in the removal of metal contaminants

Surface modified cellulose adsorbent	Heavy metals	Adsorption capacity (mg/g)	Morphological analytic features	Mechanism	References
Cellulose nano-gel	Cadmium	595.92	The microcrystalline nature was characterized through field emission scanning electron microscopy (FESEM), high-resolution transmission electron microscopy (HRTEM), XRD and the presence of functional entities through FTIR	Both the pseudo-first-order and pseudo-second-order kinetic model follows with the Freundlich isotherm model. The reaction was dominated by surface interaction and particle diffusion	El-Naggar et al. (2018)
Cellulose modified with tetrafluoroterephthalonitrile	Copper	17.94	The microcrystalline and porous nature was determined through SEM, BET (88.32 m ² /g) and the functional entities are determined through FTIR	Pseudo-second-order kinetics model and Langmuir isotherm model was followed and the reaction was dominated by electrostatic interactions and diffusion mechanism	Cao et al. (2017)
Cellulose grafted with hydroxyapatite and polyacrylamide hydrogel	Copper	93.60	The coarse nature and micro-cracks are observed through SEM and the functional entities are observed through FTIR	Pseudo-second-order kinetics model was determined and the reaction was dominated by the strong surface interactive forces	Saber-Samandari et al. (2013)
Cellulose modified with polyethylene amine	Copper	102.25	The functional entities are characterized by FTIR	Pseudo-second-order kinetics model and the Langmuir isotherm model are followed, and the reaction was dominated by surface interactions	Tang et al. (2013)
Modified cellulose with the amino grouped polyamide molecules	Copper, lead	137.48, 152.86	The crystal nature and functional entities of the compound are studied by FTIR, NMR, TGA, SEM, XPS and zeta potential	The Phenomena follows pseudo-second-order reaction and Langmuir isotherm model. The reaction was dominated through electrostatic interaction and hydrogen bonding	Kong et al. (2020)

Table 7 Zeolites used in the removal of noxious dyes

Zeolite – low-cost adsorbent	Dye molecules	Adsorption capacity (mg/g)	Morphological analytical features	Mechanism	References
Moroccan Illitic	Methylene blue	13.98	The functional entities and the crystalline nature was evaluated through FTIR and XRD	Pseudo-second-order kinetics model and the Langmuir isotherm model are followed, and the reaction was dominated by electrostatic binding interactions	Chang et al. (2016)
Zeolite	Congo red	4.30	The crystalline three-dimensional structure was determined through SEM and XRD	Pseudo-second-order kinetics model and Freundlich isotherm model are followed, and the reaction was dominated by intraparticle diffusion mechanism	Vimonses et al. (2009)
Zeolites	Basic red 46	8.56	The functional entities are evaluated through FTIR	Freundlich isotherm model was followed, and the reaction was dominated by surface interactions between the molecules	Karadag et al. (2007)
Hexadecyl trimethyl ammonium bromide—Zeolite	Reactive black 5	60.60	–	Pseudo-second-order kinetics model and the Langmuir isotherm model are followed, and the reaction was dominated by electrostatic binding interactions	Armagan et al. (2011)
CTAB- Clinoptilolite	Reactive yellow 176	5.50	The functional entities are evaluated through FTIR	Freundlich isotherm model was followed, and the reaction was dominated by surface interactions	Karadag et al. (2007)

Table 8 Zeolites used in the removal of metal contaminants

Low-cost adsorbents	Heavy metals	Adsorption capacity (mg/g)	Morphological analytic features	Mechanism	References
Natural zeolite associated with activated carbon	Cadmium, nickel	129.30 and 132.10,	The nature of the particle was analysed through XRD	Pseudo-second-order kinetics model and Freundlich isotherm model are followed, and the reaction was dominated by surface interactions	Dal Bosco et al. (2005)
Zeolite treated with glutamic acid	Cobalt	29.38	Nature and pore size of the particle was analysed through SEM, XRD, BET and TGA	Pseudo-second-order kinetics model and Langmuir isotherm model are followed, and the reaction was dominated by electrostatic binding	Borandegi and Nezamzadeh-ejhtieh (2015)
Zeolite 4A	Zinc, chromium	40.40 and 56.40,	The nature of the particle was analysed through XRD	Pseudo-second-order kinetics model and the Langmuir isotherm model are followed, and the reaction was dominated by electrostatic binding interactions	Hui et al. (2005)
Clinoptilolite	Lead	78.70	The nature of the particle was analysed through XRD	Pseudo-second-order kinetics model and the Langmuir isotherm model are followed, and the reaction was dominated by electrostatic binding interactions	Bektaş and Kara (2004)
Zeolite blended with activated carbon	Copper	101.70	The nature of the particle was analysed through SEM, XRD and BET	Pseudo-second-order kinetics model and the Langmuir isotherm model are followed, and the reaction was dominated by electrostatic binding interactions	Jha et al. (2008)

mgg^{-1}) molecules through physiochemical interaction with extensive surface moieties of biochar (Aravindhan et al. 2007). Table 9 illustrates the biochar used in the removal of different dye molecules.

The physiological and morphological traits of the biochar produced from animals and plant residues act as an effective adsorbent in the removal of heavy metals from our environment (Hassan et al. 2020). Heavy metal pollutants are highly toxic substances present in the wastewater. Biochar from the peanut shell adsorbs lead ions rapidly in comparison with zinc from the contaminants. Lead ion binds with oxygen moiety present in hydroxyl, carboxyl and alcoholic entities present in the surface of biochar. They tend in the formation of metal-hydroxyl reaction as a result of cationic exchange and electronegative nature where lead with the adsorption capacity of 107 mgg^{-1} adsorbs faster than zinc with the adsorption capacity of 4.45 mgg^{-1} (Cho et al. 2017). Biochar from peanut shells via pyrolysis is utilized for the removal of arsenite As (III) and arsenate As (V) with the adsorption capacity of 4.76 mgg^{-1} . Oxygen and amino moieties enriched in biochar surface react with those metals to form a metalloid interactive complex molecule that could be removed easily by these sorbents (Sattar et al. 2019).

Biochar from rice husk, animal manure, sawdust and sugarcane straw synthesized via pyrolysis and the physiochemical trend was altered by pyrolysis temperature and feedstock based material. At the enhanced pyrolysis temperature range from 350 to 650 °C, biochar shows an enhanced adsorption capacity in the removal of metals from wastewater (Wang et al. 2020). Modified biochar from sawdust and bark was synthesized via co-pyrolysis with urea and used as a sorbent to remove cadmium with an adsorption capacity of 4 mgg^{-1} from the wastewater. The presence of aliphatic moieties such as carboxyl entity, amide I characteristics due to carbonyl and amide II feature due to carboxylate moieties tend to form chemical and hydrogen interactions with cadmium metal ions. The synergistic effect leads to provide stability of the biochar which in turn promotes enhanced removal of cadmium with an adsorption capacity of 128.7 mgg^{-1} respectively (Zhu et al. 2020).

The interaction between the biochar and the pollutant molecule was due to electrostatic interaction, hydrogen bonding between the adsorbent and adsorbate, π - π interaction. The surface entities of hydroxyl and amino have to be identified as electron donor sites promote the electrostatic and hydrogen bonding between the molecules. Presence of carboxylic, keto and nitro groups acts as the electron acceptor sites that enhance π - π interaction between the molecules (Dai et al. 2019). Based on the type of biochar and induction of surface entities, the reaction procedure varies and Table 10 illustrates the different biochar adsorbent in the removal of heavy metal contaminants.

Economic perspective of cellulose, zeolites and biochar

The cost of adsorbents plays a prominent role in the practical large scale applications. The cost of the natural zeolites was estimated by the geological survey from the US to be around US\$40—US\$900 per metric ton and synthetic zeolites to be around US\$100—US\$2,000,000 per metric ton. The annual production of cellulose was estimated to be around 7.5×10^{10} tons (Abdul Khalil et al. 2014) and the price of the activated carbon to be around US\$2.0—US\$2.2 per kg. Research exploration on the biochar based adsorbents was concentrated more for their low budget aspects of the raw material collection and design fabrication (Ng et al. 2017). The feedstock obtained from corn stocks has been accounted to be around \$75 per tonne. The cost of numerous waste was listed as wood waste \$78, sewage waste \$70 and green waste \$55 per tonne (Shackley et al. 2011).

The annual production of biochar from wheat straw biomass was accounted to be around 4, 75, 000 tonne. Also, the production of biochar from wood residues was accounted for as US\$50–682.54 (Galinato et al. 2011). This is prone to be six times cheaper than the commercial activated carbon that costs around US\$1500 per tonne (Huang et al. 2019). Natural zeolites potentially acts as vital sorbents for the cost 0.08 US\$/Kg, Bentonite for US\$/kg 0.05–0.2, Clintoptilolite for US\$/kg 0.14–0.29, chitosan molecule for US\$/kg 16.5–10 (Kausar et al. 2018). The treatment cost of the above adsorbents could be reduced substantially if the spent low-cost adsorbents could be employed and reused for the further treatment of heavy metal and toxic dye contaminants. Researchers explored the numerous studies on integrating the above adsorbents with the various nanoparticles and observed the enhanced morphological and physiological traits in the removal of those contaminants.

Merging of nanotechnology with low-cost adsorbing materials

Classification of nano-adsorbents

Nanoparticles are synthesized through different constituents such as various polysaccharides, protein molecules and polymers that increase the removal of contaminants in comparison with the other adsorbents. The various characteristic factors of the particle size, soluble nature, charge, biodegradable nature, degree of toxicity and biocompatibility play a vital role in discharging both organic and inorganic pollutants (Yi et al. 2019). Nano-adsorbents are mainly categorized under carbonaceous nanomaterial, silica-based

Table 9 Biochar used in the removal of dyes

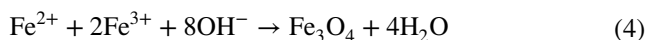
Pollutant dye molecules	Biochar	Method of Fabrication	Adsorption capacity (mg/g)	Model	References
Methylene blue	Biochar obtained from various waste residues of pinewood, pig manure and cardboard	Pyrolysis and co precipitation technique. The nature of the particle was analyzed through FTIR, XRD, BET and Zeta potential analysis	48.30	The reaction system follows the pseudo-second-order and Langmuir isotherm model	Lonappan et al. (2016)
Crystal violet	Biochar obtained from the Gliricidia sepium at the various temperature of 300 °C, 500 °C and 700 °C	Pyrolysis. The spherical nature of the particle was analyzed through FTIR, BET and EDS	125.5	The reaction follows the pseudo-second-order, Freundlich and Hill isotherm model. Electrostatic interactions and hydrogen bonding occur between the molecules	Wathukarage et al. (2019)
Direct red 141	Biochar obtained from the rice residues	Pyrolysis. The crystalline nature of the particle was analyzed through FTIR, BET, TEM and XRD	59.77	The reaction system follows the pseudo-second-order and Langmuir, Freundlich isotherm model	Chen et al. (2019)
Methylene blue	Biochar derived from date palm leaf waste residues	Simple precipitation. The nature of the particle was analyzed through FTIR, SEM, EDS	744	The reaction system follows the pseudo-second-order and Freundlich isotherm model	Shafiq et al. (2019)
Crystal violet	Biochar obtained from mushroom as the spent substrate and kelp seaweed	Co-pyrolysis. The nature of the particle was analyzed through FTIR, SEM and EDS	610.1	The reaction system follows the pseudo-second-order and Langmuir isotherm model	Sewu et al. (2017)
Methylene blue	Biochar from ramie residues	Pyrolysis. The spherical nature of the particle was analyzed through FESEM and XRD	259.27	Freundlich isotherm model and the electrostatic interactions and hydrogen bonding occur between the molecules	Gong et al. (2018)
Indosol black NF1200	Biochar derived from wood residues	Gasification. The nature of the biochar was analyzed through FTIR and SEM	185	The reaction system follows the pseudo-second-order, Langmuir and Freundlich isotherm model	Kelm et al. (2019)

Table 10 Biochar used in the removal of heavy metals

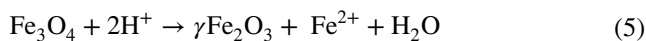
Heavy metals	Biochar	Method of Fabrication	Adsorption capacity (mg/g)	Model	References
Cadmium, nickel and copper	Biochar obtained from various waste residues of wood, animal manure	Pyrolysis technique. The nature of the particle was analyzed through FTIR, BET, SEM, EDS analysis	4, 4.14, 4.13	The reaction system follows the electrostatic and surface interactions between the molecules	Wang et al. (2020)
Arsenic	Biochar obtained from the peanut shell	Pyrolysis. The nature of the particle was analyzed through FTIR, BET, EDS and XPS	4.76	The reaction follows the pseudo-second-order and Langmuir isotherm model. Electrostatic interactions and surface complexation occur between the molecules	Sattar et al. (2019)
Cadmium, lead, copper and zinc	Biochar obtained from the Scots pine and Betula pendula	Pyrolysis. The crystalline nature of the particle was analyzed through FTIR, BET, TEM and XRD	128.7, 107, 4.49	The reaction system follows the Freundlich isotherm model	Komkiene and Baltreinaite (2016)
Copper, zinc and arsenic	Biochar derived from swine manure digestate	Pyrolysis. The nature of the particle was analyzed through FTIR, SEM, and BET	1.33, 5.33, 0.25	The reaction system follows the surface complexation, ion exchange and electrostatic interaction	Jiang et al. (2018)
Copper and lead	Biochar obtained from cotton residues	Co-pyrolysis. The nature of the particle was analyzed through FTIR, SEM, BET and EDS	145, 179	The reaction system follows the surface complexation, ion exchange and electrostatic interaction	Wang and Liu (2017)
Copper and lead,	Biochar from Olive soil residues	Pyrolysis. The nature of the particle was analyzed through FTIR and BET	0.85, 4.25	The reaction system follows the surface complexation and electrostatic interaction	Abdelhadi et al. (2017)

materials, metal or mixed metallic particles, polymer-based composites, inorganic nano-adsorbents and magnetic adsorbents (Bagheri et al. 2020). Figure 7 illustrates the schematic representation of the classification of nano-adsorbents.

Metallic nanoparticle includes metal oxide and mixed metal particles. Their main advantageous features are easy recovery, regenerating capacity, high thermal stability and the enhanced surface area owing to their porous nature (Mulenios et al. 2020). The reaction mechanistic pathway in the formation of magnetite particles is ascribed as below (Laurent et al. 2008),



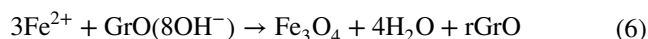
The unstable resultant magnetite obtained from the above reaction undergoes oxidation phenomena for the conversion of stable maghemite particles (Laurent et al. 2008). The reaction was ascribed as,



The demerits in the formation are an agglomeration of particle upon Vander Waals and other interactions which tends the researchers to develop a support molecule made of carbonaceous or silica or graphene materials (Xiao et al. 2019a). The carbonaceous material includes activated carbon; carbon nanotubes enhance the adsorption by formulating pi-pi interactions. Graphene molecules based on their non-covalent interactions prevent agglomeration of the nanoparticles that enhance the adsorption capacity (Guo et al. 2014).

Graphene oxide promotes electrostatic and ion-exchange interactions with pollutants owing to their numerous oxygen-rich functional moieties. Due to the

inadequate adsorption sites, reduced graphene oxide nanocomposites are preferred for their excellent electron transport viabilities. Also, the magnetic graphene composites provide adequate numerous binding areas with the strong reusable facility. To enhance the colloidal nature and stability, magnetic graphene composited with functional organic entities is substituted by researchers (Lim et al. 2018). The incorporation of metal nanoparticle with graphene molecule enhances the removal of organic pollutants and the mechanistic reaction in the formation of magnetic graphene oxide was illustrated as (Bagherzadeh et al. 2015),



Chitosan molecule for their unique characteristics feature of compatible and biodegradable nature upon the combination with the plant extracts acts as the prominent biosorbent and has shown the excellent removal of noxious dyes. The removal efficiency increased due to the electrostatic interaction and hydrogen bonding between the three-dimensional network channel of the adsorbent and the complex dye molecules (Noreen et al. 2020). Mesoporous silica particles and aerogels are categorized under silica nanoparticles. The unique functional group silanol and surface property of silica particles enhance the adsorption process upon surface complexation process (Jawed et al. 2020). The polymer-based composites enhance the adsorption process on forming the electrostatic interactions, surface complexation and ion exchange mechanisms. The adsorption purely depends on the choice of material and other physiochemical attributes of thermal stability, pH and temperature (Ge et al. 2012).

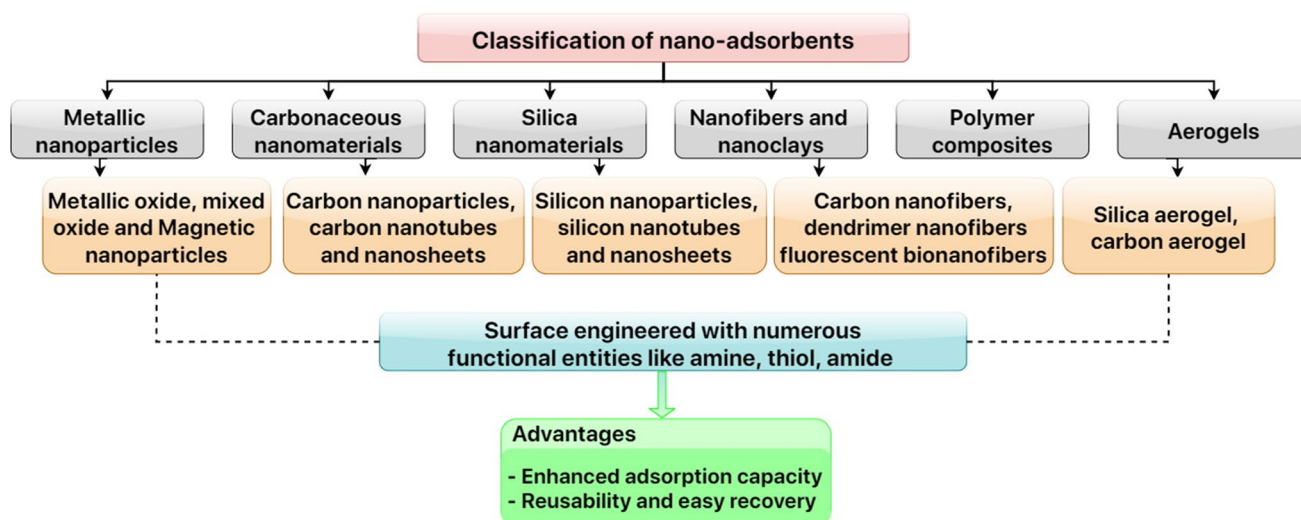


Fig. 7 Classification of nano-adsorbents surface engineered with different functional entities and their advantages

Nanoparticles as an adsorbing material in the discharge of pollutants

The facile advantageous feature of the nanoparticles is listed as low cost, homogenous size and shape, devoid of aggregating nature with enhanced stability, the enhanced surface to volume ratio and purity (Jadoun et al. 2020). These unified characteristic features urge the researchers to use them in a wide range of numerous applications of drug delivery systems, wastewater treatment, bio-instrumental application and also in the biosensor fabrications (Gopinath et al. 2020). Recently, metallic nanoparticles synthesized from iron, titanium, gold, copper, cobalt, lead and zinc oxide nanoparticles are the considerable adsorbing materials fabricated to discharge the noxious dyes from the industrial effluents.

Zero-valent iron nanoadsorbent processed with the chemical (borohydride) reduction methods is widely used to treat azo dyes released from industrial waste streams. Perhaps the magnetic nanocellulose possesses numerous hydroxyl entities and negative moieties such as carboxyl and sulphate unit promote electrostatic binding between the cationic dye pollutants and adsorbent. Anionic dye molecules could be removed upon inducing positive amine group on the surface of the nanocellulose where it provokes the strong interaction between the amino and dye molecules (Varghese et al. 2019; Yu et al. 2020). The zero-valent iron adsorbents are also prominently used in them or in discharging the pernicious vat green dye from the toxic water contaminated medium.

The graphene oxide nanocomposites and the hydroxyl entity present on their surface provoke the chemical interaction between the complex dye molecules (Methylene blue) that results in the enhanced adsorption capacity of 751.88 mgg^{-1} (Zaman et al. 2020). The hematite iron derivatives ($\alpha\text{-Fe}_2\text{O}_3$) with the magnetite iron derivatives (Fe_3O_4), aka-gaeneite ($\beta\text{-Fe}_2\text{O}_3$) and maghemite ($\gamma\text{-Fe}_2\text{O}_3$) iron derivatives possess excellent superparamagnetic behaviour with high catalytic activity and these properties are studied by many researchers (Shanehsaz et al. 2015). So they are prominently considerable to be the powerful nano-adsorbents that could remove many hazardous dye molecules (methylene blue with an adsorption capacity of 959.5 mgg^{-1} and methyl orange with an adsorption capacity of 849.3 mgg^{-1}) in the aquatic system Yavari et al. 2016; Homaeigohar 2020). Table 11 represents the various nanoparticles used in discharging the hazardous dye molecules.

The external surface of the magnetic nanoparticles is modified by numerous components, such as microorganisms, polymers and plant extracts that could be preferred as the potent adsorbents in the removal of toxic heavy metals from the industrial effluents. Table 10 gives information about heavy metal removal by magnetic nanoparticles. The nanoparticles impregnated with the various plant constitutional extracts were considered as an emerging approach in the adsorbent fabrication, and it was advantageous by reducing the emission of other secondary toxicants to the ecosystem (Vishnu and Dhandapani 2020; Vishnu et al. 2019). The superparamagnetic characteristic feature with the highly stable nature, made many researchers focus on the reinforcement of iron oxide nanoparticles (Xiao et al. 2019a; Bouhrara et al. 2011).

In numerous metal removal studies, magnetic nanoparticle was coated with silica molecule on their surface that mainly enhances the stable nature of the particle (Deng et al. 2005). Graphene molecule acts as the prominent support molecule and upon covalent and surface interactions with the magnetic particles proves to be the potent adsorbent in the removal of metal contaminants (Guo et al. 2014). Chitosan as the polymer-based support molecule acts as the robust adsorbent on fascinating the surface complex interactions with the solute molecules that solely enhance the adsorption capacity (Xiao et al. 2019a). Overall, the magnetic biochar fabricated in the magnetic medium through pyrolysis or chemical precipitation (Huang et al. 2019) shows the promising adsorbing features of both heavy metals and the dye molecules (Li et al. 2020b).

Various hybrid nanomaterial as an adsorbing material in discharging the heavy metals and dyes

The prominent advantage of nano-adsorbents is preferred for their extensive surface area and intraparticle diffusion of adsorbate inside the pores of the adsorbing materials. The nanosize of the adsorbent fascinates the numerous active sites that enhance the adsorptive capacity of metal and dyes (Mashkoor et al. 2020). The versatile nature of surface modification of the different nanomaterials with the various functional entities has gained more visibility among the researchers because of their enhanced performance in terms of adsorption capacity, stability, modified porous nature and increased surface area to volume ratio (Brião et al. 2020).

The cointegration of cobalt and ferrite nanoparticles upsurges the magnetic saturation feature which enhances the superparamagnetic behaviour of a material. The mechanism was ascribed as (Hosni et al. 2017)

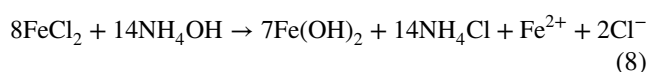
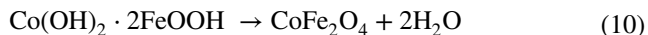
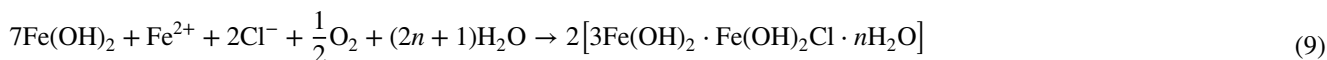


Table 11 Nanoparticles used in the removal of dyes

Pollutant dye molecules	Nanoparticle as adsorbents	Method of Fabrication	Adsorption capacity (mg/g)	Model	References
Acid blue 92	Cobalt integrated Ferrite metallic nano-adsorbents	Simple precipitation. The nature of the particle was analyzed through FTIR, XRD, BET and Zeta potential analysis	625	The reaction system follows the pseudo-second-order and Langmuir isotherm model	Yavari et al. (2016)
Brilliant green	Mn-integrated Ferrrous nanomaterial impregnated with activated carbon	Mixed reaction. The spherical nature of the particle was analyzed through FESEM and XRD	101.22	The reaction follows the Langmuir isotherm model and the electrostatic interactions and hydrogen bonding occurs between the molecules	Asfaram et al. (2017)
Bromophenol blue	Sorel's cement as nano-adsorbents	Sol-Gel technique. The crystalline nature of the particle was analyzed through TEM and XRD	4.88	The reaction system follows the pseudo-second-order and Langmuir isotherm model	El-Gamal et al. (2015)
Direct green 6, and direct red 80	Cobalt integrated Ferrite nano-adsorbent	Simple precipitation. The nature of the particle was analyzed through FTIR, XRD, BET and Zeta potential analysis	384.61, and 333.33	The reaction system follows the pseudo-second-order and Langmuir isotherm model	Yavari et al. (2016)
Malachite green	Iron nanoadsorbent impregnated on the ash compound	Co-precipitation. The nature of the particle was analyzed through FTIR and SEM	210.31	The reaction system follows the pseudo-second-order and Langmuir isotherm model	Agarwal et al. (2016)
Malachite green	Mn-doped with iron nanoparticle impregnated with activated carbon	Mixed reaction. The spherical nature of the particle was analyzed through FESEM and XRD	87.57	Langmuir isotherm model and the electrostatic interactions and hydrogen bonding occur between the molecules	Asfaram et al. (2017)
Methyl orange	Sorel's cement as nanoadsorbent	Sol-Gel. The crystalline nature of the particle was analyzed through TEM and XRD	23.21	The reaction system follows the pseudo-second-order and Langmuir isotherm model	El-Gamal et al. (2015)
Methylene Blue	Copper particles as nanoadsorbent	Precipitation. The crystalline nature of the particle was analyzed through TEM and XRD	95	The reaction system follows the pseudo-second-order and Langmuir isotherm model	El-Gamal et al. (2015)
Reactive blue 19	Magnetic nanoparticle surface coated with Polypyrrole	Co-precipitation. The spherical nature of the particle was analyzed through SEM and FTIR	112.36	The reaction system follows the pseudo-second-order and Langmuir isotherm model	Shanehsaz et al. (2015)
Methylene blue, and congo red	Carbon Nanotubes and Graphene Nanoplates	TEMPO mediated Oxidation. The nature of the particle was analyzed through FESEM and FTIR	1178.5, 585.3	The reaction system follows the pseudo-second-order and Langmuir isotherm model	Yu et al. (2020)
Methylene blue	Graphene oxide nanocomposites	The graphene nanocomposites were prepared via Coprecipitation and their characterization was observed through FTIR, SEM, TEM, XRD, BET and Zeta potential	751.88	The reaction system follows pseudo-second-order and Langmuir, Freundlich isotherm model	Zaman et al. (2020)



Cobalt ferrite nanocrystals annealed from hydroxide complex of cobalt hydroxide and iron oxyhydroxide compound. The refined advanced feature comparable to iron particles is due to the existence of primitive reactive phase of CoFe_2O_4 and subsidiary products of $\beta\text{-Fe}_2\text{O}_3$ and CoO_2 respectively (Hosni et al. 2017). Graphene nanomaterials due to their honeycomb network feature are readily categorized as the oxidative and reduced graphene oxide. The vital functional entities of carbonyl and epoxy groups constitute a prominent role in the removal of dyes and various heavy metals (Ahlawat et al. 2020; Noormohamadi et al. 2018).

Multiwalled carbon nanocomposites promote pi–pi interaction between the double bond carbon atoms in the complex dye molecule. Hydrogen interaction was because of entities such as amide, hydroxyl and carboxyl entities and electrostatic binding occurred with a negative group of nanocomposites and methylene blue dyes with an adsorption capacity of 232.5 mgg^{-1} and hydronium entities attract anionic methylene orange dyes with an adsorption capacity of 106.3 mgg^{-1} (Ahlawat et al. 2020).

Silica nanoparticles are studied by the researchers in recent years owing to their unique hydroxyl groups at their exterior surface (Li et al. 2020a; Jawed et al. 2020). The mesoporous silica particles are prone to remove a certain group of metals and dyes from the contaminated wastewater. However, due to their low colloidal property, the aggregation of particle depletes the total surface area, resulted in the reduced adsorption capacity of some metals and dyes. So the particles are incorporated with iron and other substances to increase the porosity and surface area from $638.13 \text{ m}^2\text{g}^{-1}$ to $1021.15 \text{ m}^2\text{g}^{-1}$, pore volume from $5.98 \text{ cm}^3\text{g}^{-1}$ to $6.58 \text{ cm}^3\text{g}^{-1}$ that enhances the adsorption efficiency (Shao et al. 2020; Jadhav et al. 2019).

Hydrogels act as the carrier molecules and are used in the tissue engineering and drug delivery systems. Researchers have evaluated the hybridization of carboxymethyl cellulose nanocrystals with the redox hydrogel in discharging the hazardous dye molecules. Cysteine supplies amino entity when used as an extensive crosslinking agent in the hydrogel, promotes reaction with the carboxyl groups and upon reacting with the sulphide groups it forms a strong disulphide bond with hydrogels (Crini et al. 2019b). This redox interactive hydrogels act as the robust adsorbent in removing strong organic dyes from the ecosystem (Li et al. 2020c). Cellulose nanomaterial modified with the polymerization of N-isopropyl acrylamide molecule cross-reacted with the phytic acid synthesized at the optimum pH and temperature has

proven to be the potent sorbent in the removal of lead ions with an adsorption capacity of 323.5 mgg^{-1} in both the batch and continuous system. The carboxyl groups present on the surface of the sorbent relatively show enhanced interaction with the lead ion.

Graphene molecule upon oxidation produces extensive functional entities such as carboxyl, amino and hydroxyl groups. Though the chemical feature of sporopollenin, a macro compound was still profounded by researchers, it was proven to be an adsorbent in the removal of metallic contaminants. Wide extensive research was done on combining the magnetic modified sporopollenin with graphene oxide entities and was supplied with the amino group to treat metal pollutants. The additional entity of $-\text{NH}_2$ promotes adsorption of lead whereas, magnetic sporopollenin prevents oxidation of iron particles and retains their magnetic nature under acidic nature (Marcelo et al. 2020).

The magnetic biochar when impregnated with zinc sulphide nanocrystals it shows the excellent adsorption capacity of lead (367.65 mgg^{-1}) with the prominent regenerating capability due to the presence of superparamagnetic features. The zinc nanocomposites promote surface interaction with the extensive porous surface area and form complexes with metal ions (Yan et al. 2015). The magnetic biochar nanocomposites generated from the sewage sludge and wood chips were fabricated through co-precipitation technique at two distinct temperature acts as the potent adsorbent in the removal of both hexavalent chromium ions with an adsorption capacity of 80.96 mgg^{-1} and acid orange 7 dye molecules with an adsorption capacity of 110.27 mgg^{-1} . The electrostatic interactive occurs between chromate molecule with a hydroxyl group and surface interaction promotes the binding of complex dyes with magnetic biochar (Santhosh et al. 2020). Table 12 evaluates the role of functionalized nanomaterials with the different nanomaterials in discharging the hazardous metals and dye molecules.

It could be inferred that the nanoparticle when integrated with the other molecules shows the altered morphological traits. The prominent observations are done through the numerous characterization techniques alike Fourier transforms infrared spectroscopy (FTIR), scanning electron microscope (SEM), transmission electron microscope (TEM), energy dispersive spectroscopy (EDX), Brunauer–Emmett–Teller (BET), X-Ray Diffraction (XRD) and X-ray photoelectron spectroscopy (XPS). The particular functional moieties of the hydroxyl group, carboxyl group, thiol group, amino group which enhances the electrostatic/ionic/covalent/ interactions combined with the hydrogen bonding interactions upon the aromatic dye components and

Table 12 Nanoparticles used in the removal of metal contaminants

Heavy metal	Metallic nanoparticle	Method of preparation	Adsorption capacity (mg/g)	Model	References
Copper	Magnetic chitosan biochar	Co-precipitation. The nature of the particle was analysed through FTIR, SEM, TEM and XRD	54.68	The reaction system follows the pseudo-second-order and Freundlich isotherm model	Xiao et al. (2019a)
Copper	Integrated magnetic particles with <i>Muraya koenigii</i> plant extract	Co-precipitation. The nature of the particle was analysed through FTIR, FESEM and Vibrating sample magnetometry (VSM)	73.71	The reaction system follows the pseudo-second-order and Langmuir isotherm model	Vishnu et al. (2019)
Lead	Magnetic nanoparticle integrated with EDTA	Hydrothermal. The nature of the particle was analysed through FTIR, FESEM and XRD	146.84	The reaction system follows the pseudo-second-order and Langmuir isotherm model	Wang and Wang (2018)
Hexavalent chromium	Amino-functionalized magnetic graphene	Co-precipitation. The nature of the particle was analysed through FTIR, SEM, TEM, BET and XRD	17.29	The reaction system follows the pseudo-second-order and Freundlich isotherm model	Guo et al. (2014)
Hexavalent chromium	Ferrous magnetic particle integrated with biochar	Hydrothermal. The nature of the particle was analysed through FTIR, SEM, TEM and XRD	30.14	The reaction system follows the pseudo-second-order and Freundlich isotherm model	Xiao et al. (2019a)
Zinc	Polymers integrated with the magnetic nanoparticle	Co-precipitation. The nature of the particle was analysed through FTIR, TGA, TEM and XRD	39.40	The reaction system follows the pseudo-second-order and Langmuir isotherm model	Ge et al. (2012)

Table 13 Surface modified nanoparticles used as the adsorbing materials in discharging the organic and inorganic contaminants

Functionalized nanomaterial	Removal of dyes and metals	Merits	References
Cobalt- ferrite integrated with silica polyethyleneimine magnetic nanoparticles	Tartrazine—an azo dye prominently used in food industries	Removal efficiency is about 99.5% and reused for 8 continuous cycles	Noormohamadi et al. (2018)
Silica integrated with a starch composite	Methylene blue and crystal violet—cationic dyes and copper metal	Removal of three pollutants with the enhanced adsorption capacities of 653.21, 1246.4 and 383.08 mg/g, respectively	Li et al. (2020a)
Nickel coated magnetized nanocomposites doped with sucrose molecules	Malachite green	The calculated magnetic capability was evaluated around 87.7 mg/g determined with electrostatic interactions and weaker hydrogen binding upon dye molecules respectively. Reusable for 5 cycles	Mohanta et al. (2020)
Silica nanoparticle immobilized with <i>Paecilomyces lilacinus</i>	Lead—Heavy metal	The enhanced adsorption capacity of 282.49 mg/g	Ruan et al. (2019)
Magnetic ferrous nanoparticle immobilized with 1,2,4,5-Benzenetetracarboxylic acid	Congo red, methylene blue and crystal violet	The enhanced adsorption capacity for Congo red – 630 mg/g and reusable for 5 cycles	Chatterjee et al. (2020)
Calcium silicate hydrate	Copper, nickel, zinc and chromium	Enhanced adsorption of 100 mg/g for all these metals	Shao et al. (2020)
Multiwalled carbon nanotubes impregnated with activated carbon	Methylene blue and methyl orange—Cationic and anionic dyes	The enhanced absorptive capacity of 232.5 mg/g was observed	Ahlawat et al. (2020)
Magnetic carbonaceous adsorbent	Methylene blue	The enhanced absorptive capacity of 500 mg/g was obtained	Li et al. (2020d)
Magnetic silica layered graphene nanocomposite	Lead ions	The nanocomposite was synthesized via the combined method of copolymerization and crosslinking. Batch mode was used in the removal of lead ions with the maximum adsorption capacity of 323.5 mg/g	Mohd et al. (2020)
Magnetic cobalt ferrite nanoparticle	Caesium ions	The enhanced absorptive capacity of 178.8 mg/g was detected	Li et al. (2020d)
Cobalt iron oxide nanoparticles	Anionic azo dyes (Amaranth, acid orange 7, naphthol blue-black, reactive orange 16, acid orange 52 and reactive red)	The removal efficiency of 98.9% was obtained with the reusability of 5 cycles	Qurrat-Ul-Ain et al. (2019)
Polymer functionalized magnetic nanoparticle	Mercury and lead	Removal capability of 294.61 mg/g and 198.2 were obtained with the reusability of 7 cycles	Ahamad et al. (2020)
Magnetic biochar impregnated with zinc sulphide	Lead	The removal adsorption capacity of lead 367.65 mg/g	Yan et al. (2015)
Magnetic biochar nanocomposites impregnated with different types of sewage sludge and woodchips	Hexavalent chromium and acid orange 7	The removal adsorption capacity of 80.96 mg/g and 110.27 mg/g with the recycling ability of five consecutive cycles	Santhosh et al. (2020)

metal ion complexes. The bimetallic nano-adsorbents with the altered functional entities promote the enhanced adsorption capacity with the advantageous feature of recovery and reusability (Vishnu et al. 2020).

Perspective

Hybridized nano-adsorbents act as the robust and prominent adsorbent in the removal of dual inorganic and organic contaminants from the aquatic systems. Though numerous treatment technologies of physical, chemical and physio-chemical methods cleanse the organic and inorganic pollutants, adsorption is primitively preferred by major researchers owing to their production cost and design simplicity. The huge quantity of adsorbing materials is generated and utilized in discharging both the organic and inorganic pollutants using adsorption technique. Nanomaterials are extensively considered in the numerous applications owing to their advantageous feature of size and considerable surface area with volume ratio. Magnetic materials, reduced to the nanosize, are generated as an adsorbent to fill the gap of reusing adsorbent for numerous cycles (Table 13).

The integrated approach of sustainable magnetic nanoparticles with the surface engineered entities plays a pivotal role in the environmental remediation aspects. They act as the great support and carrier molecules on the removal of both organic and inorganic contaminants. Many researchers are still exploiting on developing the specific adsorbent used for the discharge of multiple organic and inorganic pollutants. The consequence of the usage of modifiers that alters the surface functional traits should be explored more by the researchers. The numerous adsorption mechanism of the nano-adsorbents in the removal of various organic and inorganic contaminants should be explored in detail. The catalytic degradation ability of the magnetic nano-adsorbents in the removal of organic dye molecules has to be focused more by the researchers. The usage of the spent adsorbents after adsorption phenomena is the greatest disadvantage and the researchers need to focus more on them. Since water is a vital resource for all the floral organisms in our ecosystem, developing a safe and advantageous cost-effective treatment technique is necessary to protect our environment.

Conclusion

The toxic heavy metal and complex dye removal from the wastewater effluents are embarked as the most vital treatment in environmental protection. The improved urbanization and the desire of mankind to move towards modernization result in the accumulation of various organic and inorganic pollutants in the environment. The prolonged

accumulated pollutants impact all the organisms in our ecological community. The current comprehensive review had listed the distinct conventional and non-conventional treatment technologies on the eradication of these organic and inorganic pollutants. These technologies ignite the target of remodelling the water quality that helps to attain a cleaner environment. Many countries around the world are still incompetent to adopt the apt treatment strategy due to the lack of appropriate equipment design, high production, manufacturing and operational cost. On enabling the appropriate modern and viable treatment strategy in the large-scale implementation, the pros and cons of the application challenges should be strongly considered and analysed to proceed further. Adsorption is still considered as the essential strategy in the purification of aquatic systems that are greatly polluted with the numerous heavy metals and hazardous dye contaminants.

The consecutive accumulation of the various pollutants tends the researchers to develop the various adsorbents of low cost from the different waste residues. In this review, we had briefly explained about the low-cost adsorbents and nano-adsorbents used in the removal of metal and dye contaminants. These vital adsorbents promote the enhanced removal of both the inorganic heavy metal as well as the organic dyes from the contaminated wastewater. The disadvantage of the low-cost adsorbent tends the researchers to develop the various nano-adsorbents from distinct materials that fill the gap of recovery and reusability. We have extensively compared and listed the advantages of using nano-adsorbents from low-cost adsorbents in the environmental remediation aspect of metal and complex dye removal. The boom of nano-adsorbents develops numerous advantages for large-scale industries.

Advancement on the integrated nanoparticle towards green approach prominently reduces the emission of secondary toxicants to the ecosystem. Researchers have intended in the synthesis of hybridized nanomaterials and integrating it with the various functional entities on their surface molecules. The enhanced efficacy upon their surface modification with the change in the morphological traits had also been illustrated. The classification of nano-adsorbents and their influence on inducing them with the various functional entities are also discussed. The future research has the scope to develop the distinct nano-adsorbents in the low cost and to use it in the industrial applications with improved efficiency. To attain the aquatic system to be freed from such hazardous metal and dye pollutants, researchers should tend to provide a promising solution with the extended technologies by addressing the current pertaining challenges.

Acknowledgements Authors are grateful to SSN Trust, India for financial support.

Compliance with ethical standards

Conflict of interest The authors declare that they have no conflict of interest.

References

- Abd El-Rahim WM, Moawad H, Abdel Azeiz AZ, Sadowsky MJ (2017) Optimization of conditions for decolorization of azo-based textile dyes by multiple fungal species. *J Biotechnol* 260:11–17. <https://doi.org/10.1016/j.jbiotec.2017.08.022>
- Abdelbasir SM, Shalan AE (2019) An overview of nanomaterials for industrial wastewater treatment. *Korean J Chem Eng* 36:1209–1225. <https://doi.org/10.1007/s11814-019-0306-y>
- Abdelhadi SO, Dosoretz CG, Rytwo G et al (2017) Production of biochar from olive mill solid waste for heavy metal removal. *Bioresour Technol* 244:759–767. <https://doi.org/10.1016/j.biortech.2017.08.013>
- Abdul Khalil HPS, Davoudpour Y, Islam MN et al (2014) Production and modification of nanofibrillated cellulose using various mechanical processes: A review. *Carbohydr Polym* 99:649–665. <https://doi.org/10.1016/j.carbpol.2013.08.069>
- Agarwal S, Tyagi I, Gupta VK et al (2016) Kinetics and thermodynamics of Malachite Green dye removal from aqueous phase using iron nanoparticles loaded on ash. *J Mol Liq* 223:1340–1347. <https://doi.org/10.1016/j.molliq.2016.04.039>
- Ahamad T, Naushad M, Alshehri SM (2020) Journal of Water Process Engineering Fabrication of magnetic polymeric resin for the removal of toxic metals from aqueous medium: Kinetics and adsorption mechanisms. *J Water Process Eng* 36:101284. <https://doi.org/10.1016/j.jwpe.2020.101284>
- Ahlawat W, Kataria N, Dilbaghi N et al (2020) Carbonaceous nanomaterials as effective and efficient platforms for removal of dyes from aqueous systems. *Environ Res* 181:108904. <https://doi.org/10.1016/j.envres.2019.108904>
- Al-Ghouti MA, Da'ana DA (2020) Guidelines for the use and interpretation of adsorption isotherm models: A review. *J Hazard Mater* 393:122383. <https://doi.org/10.1016/j.jhazmat.2020.122383>
- Al-Ghouti MA, Razavi MM (2020) Water reuse: Brackish water desalination using *Prosopis juliflora*. *Environ Technol Innov* 17:100614. <https://doi.org/10.1016/j.eti.2020.100614>
- Allen SJ, McKay G, Porter JF (2004) Adsorption isotherm models for basic dye adsorption by peat in single and binary component systems. *J Colloid Interface Sci* 280:322–333. <https://doi.org/10.1016/j.jcis.2004.08.078>
- Aravindhan R, Rao JR, Nair BU (2007) Removal of basic yellow dye from aqueous solution by sorption on green alga *Caulerpa scalpelliformis*. *J Hazard Mater* 142:68–76. <https://doi.org/10.1016/j.jhazmat.2006.07.058>
- Arefi Pour A, Sharifnia S, Neishabori Salehi R, Ghodrati M (2016) Adsorption separation of CO₂/CH₄ on the synthesized NaA zeolite shaped with montmorillonite clay in natural gas purification process. *J Nat Gas Sci Eng* 36:630–643. <https://doi.org/10.1016/j.jngse.2016.11.006>
- Armagan B, Turan M, Karadag D (2011) Adsorption of different reactive dyes onto surfactant-modified zeolite: kinetic and equilibrium modeling. *Surviv Sustai*. <https://doi.org/10.1007/978-3-540-95991-5>
- Asfaram A, Ghaedi M, Hajati S et al (2017) Screening and optimization of highly effective ultrasound-assisted simultaneous adsorption of cationic dyes onto Mn-doped Fe₃O₄-nanoparticle-loaded activated carbon. *Ultrason Sonochem* 34:1–12. <https://doi.org/10.1016/j.ultsonch.2016.05.011>
- Ayawei N, Ebelegi AN, Wankasi D (2017) Modelling and interpretation of adsorption isotherms. *J Chem*. <https://doi.org/10.1155/2017/3039817>
- Azari A, Nabizadeh R, Nasser S et al (2020) Comprehensive systematic review and meta-analysis of dyes adsorption by carbon-based adsorbent materials: Classification and analysis of last decade studies. *Chemosphere* 250:126238. <https://doi.org/10.1016/j.chemosphere.2020.126238>
- Badruddoza AZM, Tay ASH, Tan PY et al (2011) Carboxymethyl-β-cyclodextrin conjugated magnetic nanoparticles as nano-adsorbents for removal of copper ions: Synthesis and adsorption studies. *J Hazard Mater* 185:1177–1186. <https://doi.org/10.1016/j.jhazmat.2010.10.029>
- Bagheri H, Fakhri H, Ghahremani R et al (2020) Nanomaterial-based adsorbents for wastewater treatment. *Elsevier Tech*. 28:467–485. <https://doi.org/10.1016/b978-0-12-816770-0.00028-9>
- Bagherzadeh M, Amrollahi MA, Makizadeh S (2015) Decoration of Fe₃O₄ magnetic nanoparticles on graphene oxide nanosheets. *RSC Adv* 5:105499–105506. <https://doi.org/10.1039/c5ra22315f>
- Bashir A, Malik LA, Ahad S et al (2019) Removal of heavy metal ions from aqueous system by ion-exchange and biosorption methods. *Environ Chem Lett* 17:729–754. <https://doi.org/10.1007/s10311-018-00828-y>
- Bektaş N, Kara S (2004) Removal of lead from aqueous solutions by natural clinoptilolite: Equilibrium and kinetic studies. *Sep Purif Technol* 39:189–200. <https://doi.org/10.1016/j.seppur.2003.12.001>
- Borandegi M, Nezamzadeh-ejhieh A (2015) Colloids and Surfaces A : Physicochemical and Engineering Aspects Enhanced removal efficiency of clinoptilolite nano-particles toward Co (II) from aqueous solution by modification with glutamic acid. *Colloids Surfaces A Physicochem Eng Asp* 479:35–45. <https://doi.org/10.1016/j.colsurfa.2015.03.040>
- Bouhrara M, Polshettiwar V, Basset J-M et al (2011) Magnetically recoverable nanocatalysts. *Chem Rev* 111:3036–3075. <https://doi.org/10.1021/cr100230z>
- de Brião GV, de Andrade JR, da Silva MGC, Vieira MGA (2020) Removal of toxic metals from water using chitosan-based magnetic adsorbents. *A Rev Environ Chem Lett* 18:1145–1168. <https://doi.org/10.1007/s10311-020-01003-y>
- Cai Z (2020) Remediation of soil and groundwater contaminated with organic chemicals using stabilized nanoparticles: lessons from the past two decades. *Front Environ Sci Eng* 14:1–19
- Cao F, Lian C, Yu J et al (2019) Study on the adsorption performance and competitive mechanism for heavy metal contaminants removal using novel multi-pore activated carbons derived from recyclable long-root *Eichhornia crassipes*. *Bioresour Technol*. <https://doi.org/10.1016/j.biortech.2019.01.007>
- Cao J, Fei D, Tian X et al (2017) Novel modified microcrystalline cellulose-based porous material for fast and effective heavy-metal removal from aqueous solution. *Cellulose* 24:5565–5577. <https://doi.org/10.1007/s10570-017-1504-6>
- Chang J, Ma J, Ma Q et al (2016) Adsorption of methylene blue onto Fe₃O₄/activated montmorillonite nanocomposite. *Appl Clay Sci* 119:132–140. <https://doi.org/10.1016/j.clay.2015.06.038>
- Chao X, Qian X, Han-hua Z et al (2018) Effect of biochar from peanut shell on speciation and availability of lead and zinc in an acidic paddy soil. *Ecotoxicol Environ Saf* 164:554–561. <https://doi.org/10.1016/j.ecoenv.2018.08.057>
- Chatterjee S, Guha N, Krishnan S et al (2020) Selective and recyclable congo red dye adsorption by spherical Fe₃O₄ nanoparticles functionalized with 1,2,4,5-benzenetetracarboxylic acid. *Sci Rep* 10:1–11. <https://doi.org/10.1038/s41598-019-57017-2>

- Chen S, Qin C, Wang T et al (2019) Study on the adsorption of dyes with different properties by sludge-rice husk biochar: adsorption capacity, isotherm, kinetic, thermodynamics and mechanism. *J Mol Liq* 285:62–74. <https://doi.org/10.1016/j.molliq.2019.04.035>
- Cho DW, Kwon G, Yoon K et al (2017) Simultaneous production of syngas and magnetic biochar via pyrolysis of paper mill sludge using CO₂ as reaction medium. *Energy Convers Manag* 145:1–9. <https://doi.org/10.1016/j.enconman.2017.04.095>
- Chowdhary P, Raj A, Bharagava RN (2018) Environmental pollution and health hazards from distillery wastewater and treatment approaches to combat the environmental threats: a review. *Chemosphere* 194:229–246. <https://doi.org/10.1016/j.chemosphere.2017.11.163>
- Crini G, Lichtfouse E (2019) Advantages and disadvantages of techniques used for wastewater treatment. *Environ Chem Lett* 17:145–155. <https://doi.org/10.1007/s10311-018-0785-9>
- Crini G, Lichtfouse E, Wilson LD, Morin-Crini N (2019a) Conventional and non-conventional adsorbents for wastewater treatment. *Environ Chem Lett* 17:195–213. <https://doi.org/10.1007/s10311-018-0786-8>
- Crini G, Torri G, Lichtfouse E et al (2019b) Dye removal by biosorption using cross-linked chitosan-based hydrogels. *Environ Chem Lett* 17:1645–1666. <https://doi.org/10.1007/s10311-019-00903-y>
- Dai Y, Zhang N, Xing C et al (2019) The adsorption, regeneration and engineering applications of biochar for removal organic pollutants: a review. *Chemosphere* 223:12–27. <https://doi.org/10.1016/j.chemosphere.2019.01.161>
- Dal Bosco SM, Jimenez RS, Carvalho WA (2005) Removal of toxic metals from wastewater by Brazilian natural scolecite. *J Colloid Interface Sci* 281:424–431. <https://doi.org/10.1016/j.jcis.2004.08.060>
- Das N (2010) Recovery of precious metals through biosorption—a review. *Hydrometallurgy* 103:180–189. <https://doi.org/10.1016/j.hydromet.2010.03.016>
- Demirbas E, Kobya M, Konukman AES (2008) Error analysis of equilibrium studies for the almond shell activated carbon adsorption of Cr(VI) from aqueous solutions. *J Hazard Mater* 154:787–794. <https://doi.org/10.1016/j.jhazmat.2007.10.094>
- Deng YH, Wang CC, Hu JH et al (2005) Investigation of formation of silica-coated magnetite nanoparticles via sol-gel approach. *Colloids Surfaces A Physicochem Eng Asp* 262:87–93. <https://doi.org/10.1016/j.colsurfa.2005.04.009>
- El-Gamal SMA, Amin MS, Ahmed MA (2015) Removal of methyl orange and bromophenol blue dyes from aqueous solution using Sorel's cement nanoparticles. *J Environ Chem Eng* 3:1702–1712. <https://doi.org/10.1016/j.jece.2015.06.022>
- El-Naggar ME, Radwan EK, El-Wakeel ST et al (2018) Synthesis, characterization and adsorption properties of microcrystalline cellulose based nanogel for dyes and heavy metals removal. *Int J Biol Macromol* 113:248–258. <https://doi.org/10.1016/j.ijbiomac.2018.02.126>
- Foo KY, Hameed BH (2010) Insights into the modeling of adsorption isotherm systems. *Chem Eng J* 156:2–10. <https://doi.org/10.1016/j.cej.2009.09.013>
- Galinato SP, Yoder JK, Granatstein D (2011) The economic value of biochar in crop production and carbon sequestration. *Energy Policy* 39:6344–6350. <https://doi.org/10.1016/j.enpol.2011.07.035>
- Ge F, Li MM, Ye H, Zhao BX (2012) Effective removal of heavy metal ions Cd²⁺, Zn²⁺, Pb²⁺, Cu²⁺ from aqueous solution by polymer-modified magnetic nanoparticles. *J Hazard Mater* 211–212:366–372. <https://doi.org/10.1016/j.jhazmat.2011.12.013>
- Ghasemipanah K (2013) Treatment of ion-exchange resins regeneration wastewater using reverse osmosis method for reuse. *Desalination Water Treat* 51:5179–5183. <https://doi.org/10.1080/19443994.2013.768420>
- Ghosh A, Dastidar MG, Sreekrishnan TR (2016) Recent advances in bioremediation of heavy metals and metal complex dyes: review. *J Environ Eng (United States)*. [https://doi.org/10.1061/\(ASCE\)EE.1943-7870.0000965](https://doi.org/10.1061/(ASCE)EE.1943-7870.0000965)
- Gokulan R, Avinash A, Prabhu GG, Jegan J (2019) Remediation of remazol dyes by biochar derived from *Caulerpa scalpelliformis*—an eco-friendly approach. *J Environ Chem Eng* 7:103297. <https://doi.org/10.1016/j.jece.2019.103297>
- Gong X, Huang D, Liu Y et al (2018) Pyrolysis and reutilization of plant residues after phytoremediation of heavy metals contaminated sediments: For heavy metals stabilization and dye adsorption. *Bioresour Technol* 253:64–71. <https://doi.org/10.1016/j.biortech.2018.01.018>
- Gopinath KP, Vo DVN, Gnana Prakash D et al (2020) Environmental applications of carbon-based materials: a review. *Environ Chem Lett*. <https://doi.org/10.1007/s10311-020-01084-9>
- Goyal N, Barman S, Bulasara VK (2016) Adsorptive removal of Biochanin A, an endocrine disrupting compound, from its aqueous solution by synthesized zeolite NaA. *Desalination Water Treat* 57:20608–20618. <https://doi.org/10.1080/19443994.2015.1108872>
- Guo X, Du B, Wei Q et al (2014) Synthesis of amino functionalized magnetic graphenes composite material and its application to remove Cr(VI). *J Hazard Mater*, Pb(II), Hg(II), Cd(II) and Ni(II) from contaminated water. <https://doi.org/10.1016/j.jhazmat.2014.05.075>
- Hao Y, Cui Z, Yang H et al (2018) Adsorption of CR (VI) by cellulose adsorbent prepared using ionic liquid as a green homogeneous reaction medium. *Cellul Chem Technol* 52:485–494
- Hassan M, Liu Y, Naidu R et al (2020) Influences of feedstock sources and pyrolysis temperature on the properties of biochar and functionality as adsorbents: A meta-analysis. Elsevier, Amsterdam
- Hernández-Montoya V, Pérez-Cruz MA, Mendoza-Castillo DI et al (2013) Competitive adsorption of dyes and heavy metals on zeolitic structures. *J Environ Manage* 116:213–221. <https://doi.org/10.1016/j.jenvman.2012.12.010>
- Homaeigozar S (2020) The nanosized dye adsorbents for water treatment. *Nanomaterials* 10:1–42. <https://doi.org/10.3390/nano10020295>
- Hosni N, Zehani K, Bartoli T et al (2017) Semi-hard magnetic properties of nanoparticles of cobalt ferrite synthesized by the coprecipitation process. *J Alloys Compd* 694:1295–1301. <https://doi.org/10.1016/j.jallcom.2016.09.252>
- Hu D, Wang P, Li J, Wang L (2014) Functionalization of microcrystalline cellulose with N, N-dimethyldodecylamine for the removal of congo red dye from an aqueous solution. *BioResources* 9:5951–5962. <https://doi.org/10.15376/biores.9.4.5951-5962>
- Huang Q, Song S, Chen Z et al (2019) Biochar-based materials and their applications in removal of organic contaminants from wastewater: state-of-the-art review. *Biochar* 1:45–73. <https://doi.org/10.1007/s42773-019-00006-5>
- Huang X, Li B, Wang S et al (2020) Facile in-situ synthesis of PEI-Pt modified bacterial cellulose bio-adsorbent and its distinctly selective adsorption of anionic dyes. *Colloids Surfaces A Physicochem Eng Asp* 586:124163. <https://doi.org/10.1016/j.colsurfa.2019.124163>
- Hui KS, Chao CYH, Kot SC (2005) Removal of mixed heavy metal ions in wastewater by zeolite 4A and residual products from recycled coal fly ash. *J Hazard Mater* 127:89–101. <https://doi.org/10.1016/j.jhazmat.2005.06.027>
- Hussin MH, Pohan NA, Garba ZN et al (2016) Physicochemical of microcrystalline cellulose from oil palm fronds as potential methylene blue adsorbents. *Int J Biol Macromol* 92:11–19. <https://doi.org/10.1016/j.ijbiomac.2016.06.094>

- Iqhrammullah M, Marlina, Nur S (2020) Adsorption behaviour of hazardous dye (Methyl orange) on cellulose-acetate polyurethane sheets. In: IOP conference series: materials science and engineering 845: 012035
- Ivanković T, Hrenović J (2010) Surfactants in the environment. *Arh Hig Rada Toksikol* 61:95–110. <https://doi.org/10.2478/10004-1254-61-2010-1943>
- Jadhav SA, Garud HB, Patil AH et al (2019) Recent advancements in silica nanoparticles based technologies for removal of dyes from water. *Colloids Interface Sci Commun* 30:100181. <https://doi.org/10.1016/j.colcom.2019.100181>
- Jadoun S, Arif R, Jangid NK, Meena RK (2020) Green synthesis of nanoparticles using plant extracts: a review. *Environ Chem Lett* 18:11–20. <https://doi.org/10.1007/s10311-020-01074-x>
- Jawed A, Saxena V, Pandey LM (2020) Engineered nanomaterials and their surface functionalization for the removal of heavy metals: a review. *J Water Process Eng* 33:101009. <https://doi.org/10.1016/j.jwpe.2019.101009>
- Jha VK, Matsuda M, Miyake M (2008) Sorption properties of the activated carbon-zeolite composite prepared from coal fly ash for Ni^{2+} , Cu^{2+} , Cd^{2+} and Pb^{2+} . *J Hazard Mater* 160:148–153. <https://doi.org/10.1016/j.jhazmat.2008.02.107>
- Jiang B, Lin Y, Mbog JC (2018) Biochar derived from swine manure digestate and applied on the removals of heavy metals and antibiotics. *Bioresour Technol* 270:603–611. <https://doi.org/10.1016/j.biortech.2018.08.022>
- Karadag D, Akgul E, Tok S et al (2007) Basic and reactive dye removal using natural and modified zeolites. *J Chem Eng Data* 52:2436–2441. <https://doi.org/10.1021/je7003726>
- Kasiri MB, Safapour S (2014) Natural dyes and antimicrobials for green treatment of textiles. *Environ Chem Lett* 12:1–13. <https://doi.org/10.1007/s10311-013-0426-2>
- Kausar A, Iqbal M, Javed A et al (2018) Dyes adsorption using clay and modified clay: a review. *J Mol Liq* 256:395–407. <https://doi.org/10.1016/j.molliq.2018.02.034>
- Kelm MAP, da Silva Júnior MJ, de Barros Holanda SH et al (2019) Removal of azo dye from water via adsorption on biochar produced by the gasification of wood wastes. *Environ Sci Pollut Res* 26:28558–28573. <https://doi.org/10.1007/s11356-018-3833-x>
- Komkiene J, Baltreinaite E (2016) Biochar as adsorbent for removal of heavy metal ions [Cadmium(II), Copper(II), Lead(II), Zinc(II)] from aqueous phase. *Int J Environ Sci Technol* 13:471–482. <https://doi.org/10.1007/s13762-015-0873-3>
- Kong Q, Preis S, Li L et al (2020) Graphene oxide-terminated hyperbranched amino polymer-carboxymethyl cellulose ternary nanocomposite for efficient removal of heavy metals from aqueous solutions. *Int J Biol Macromol* 149:581–592. <https://doi.org/10.1016/j.ijbiomac.2020.01.185>
- Largitte L, Pasquier R (2016) New models for kinetics and equilibrium homogeneous adsorption. *Chem Eng Res Des* 112:289–297. <https://doi.org/10.1016/j.cherd.2016.06.021>
- Laurent S, Forge D, Port M, et al (2008) Magnetic nanoparticles : synthesis, stabilization, vectorization, physicochemical characterizations, and biological applications. Pp 2064–2110
- Li P, Gao B, Li A, Yang H (2020a) Evaluation of the selective adsorption of silica-sand/anionized-starch composite for removal of dyes and Copper(II) from their aqueous mixtures. Elsevier, Amsterdam. <https://doi.org/10.1016/j.ijbiomac.2020.02.047>
- Li X, Wang C, Zhang J et al (2020b) Preparation and application of magnetic biochar in water treatment: a critical review. *Sci Total Environ* 711:134847. <https://doi.org/10.1016/j.scitotenv.2019.134847>
- Li Y, Hou X, Pan Y et al (2020c) Redox-responsive carboxymethyl cellulose hydrogel for adsorption and controlled release of dye. *Eur Polym J* 123:109447. <https://doi.org/10.1016/j.eurpolymj.2019.109447>
- Li Y, Zimmerman AR, He F et al (2020d) Solvent-free synthesis of magnetic biochar and activated carbon through ball-mill extrusion with Fe_3O_4 nanoparticles for enhancing adsorption of methylene blue. *Sci Total Environ* 722:137972. <https://doi.org/10.1016/j.scitotenv.2020.137972>
- Lim JY, Mubarak NM, Abdullah EC et al (2018) Recent trends in the synthesis of graphene and graphene oxide based nanomaterials for removal of heavy metals—a review. *J Ind Eng Chem* 66:29–44. <https://doi.org/10.1016/j.jiec.2018.05.028>
- Lonappan L, Rouissi T, Das RK et al (2016) Adsorption of methylene blue on biochar microparticles derived from different waste materials. *Waste Manag* 49:537–544. <https://doi.org/10.1016/j.wasman.2016.01.015>
- Makvandi P, Iftekhar S, Pizzetti F et al (2020) Functionalization of polymers and nanomaterials for water treatment, food packaging, textile and biomedical applications: a review. *Environ Chem Lett*. <https://doi.org/10.1007/s10311-020-01089-4>
- Malik LA, Bashir A, Qureashi A, Pandith AH (2019) Detection and removal of heavy metal ions: a review. *Environ Chem Lett* 17:1495–1521. <https://doi.org/10.1007/s10311-019-00891-z>
- Marcelo LR, de Gois JS, da Silva AA, Cesar DV (2020) Synthesis of iron-based magnetic nanocomposites and applications in adsorption processes for water treatment: a review. *Environ Chem Lett* 18:1–46. <https://doi.org/10.1007/s10311-020-01134-2>
- Marcucci M, Ciardelli G, Matteucci A et al (2002) Experimental campaigns on textile wastewater for reuse by means of different membrane processes. *Desalination* 149:137–143. [https://doi.org/10.1016/S0011-9164\(02\)00745-2](https://doi.org/10.1016/S0011-9164(02)00745-2)
- Mashkoo F, NasarInamuddin A (2020) Carbon nanotube-based adsorbents for the removal of dyes from waters: a review. *Environ Chem Lett* 18:605–629. <https://doi.org/10.1007/s10311-020-00970-6>
- Mohanta J, Dey B, Dey S (2020) Sucrose-triggered, self-sustained combustive synthesis of magnetic nickel oxide nanoparticles and efficient removal of malachite green from Water. *ACS Omega* 5:16510–16520. <https://doi.org/10.1021/acsomega.0c00999>
- Mohd A, Aini W, Ibrahim W et al (2020) New effective 3-aminopropyl-trimethoxysilane functionalized magnetic sporopollenin-based silica coated graphene oxide adsorbent for removal of Pb(II) from aqueous environment. *J Environ Manage* 253:109658. <https://doi.org/10.1016/j.jenvman.2019.109658>
- Mulenos MR, Liu J, Lujan H et al (2020) Copper, silver, and titania nanoparticles do not release ions under anoxic conditions and release only minute ion levels under oxic conditions in water: evidence for the low toxicity of nanoparticles. *Environ Chem Lett* 18:1319–1328. <https://doi.org/10.1007/s10311-020-00985-z>
- Ng WC, You S, Ling R et al (2017) Co-gasification of woody biomass and chicken manure: Syngas production, biochar reutilization, and cost-benefit analysis. *Energy* 139:732–742. <https://doi.org/10.1016/j.energy.2017.07.165>
- Ngulube T, Gumbo JR, Masindi V, Maity A (2017) An update on synthetic dyes adsorption onto clay based minerals: a state-of-art review. *J Environ Manage* 191:35–57. <https://doi.org/10.1016/j.jenvman.2016.12.031>
- Nidheesh PV, Zhou M, Oturan MA (2018) An overview on the removal of synthetic dyes from water by electrochemical advanced oxidation processes. *Chemosphere* 197:210–227. <https://doi.org/10.1016/j.chemosphere.2017.12.195>
- Noormohamadi HR, Fat'hi MR, Ghaedi M (2018) Fabrication of polyethyleneimine modified cobalt ferrite as a new magnetic sorbent for the micro-solid phase extraction of tartrazine from food and water samples. *J Colloid Interface Sci* 531:343–351. <https://doi.org/10.1016/j.jcis.2018.07.026>
- Noreen S, Nawaz H, Iqbal M et al (2020) Chitosan, starch, polyaniline and polypyrrole biocomposite with sugarcane bagasse for

- the efficient removal of Acid Black dye. *Int J Biol Macromol* 147:439–452. <https://doi.org/10.1016/j.ijbiomac.2019.12.257>
- Paul D (2017) Research on heavy metal pollution of river Ganga: a review. *Ann Agrar Sci* 15:278–286. <https://doi.org/10.1016/j.aasci.2017.04.001>
- Pavithra KG, Jaikumar V (2019) Removal of colorants from wastewater: a review on sources and treatment strategies. *J Ind Eng Chem* 75:1–19. <https://doi.org/10.1016/j.jiec.2019.02.011>
- Perera M, Wijenayaka LA, Siriwardana K et al (2020) Gold nanoparticle decorated titania for sustainable environmental remediation: green synthesis, enhanced surface adsorption and synergistic photocatalysis. *RSC Adv* 10:29594–29602. <https://doi.org/10.1039/d0ra05607c>
- Porter JF, McKay G, Choy KH (1999) The prediction of sorption from a binary mixture of acidic dyes using single- and mixed-isotherm variants of the ideal adsorbed solute theory. *Chem Eng Sci* 54:5863–5885. [https://doi.org/10.1016/S0009-2509\(99\)00178-5](https://doi.org/10.1016/S0009-2509(99)00178-5)
- Prakash Sharma V, Sharma U, Chattopadhyay M, Shukla VN (2018) Advance applications of nanomaterials: a review. *Mater Today Proc* 5:6376–6380. <https://doi.org/10.1016/j.matpr.2017.12.248>
- Qurrat-Ul-Ain KS, Gul Z et al (2019) Anionic azo dyes removal from water using amine-functionalized cobalt-iron oxide nanoparticles: a comparative time-dependent study and structural optimization towards the removal mechanism. *RSC Adv* 10:1021–1041. <https://doi.org/10.1039/c9ra07686g>
- Ananthashankar R (2013) Production, characterization and treatment of textile effluents: a critical review. *J Chem Eng Process Technol* 05:1–18. <https://doi.org/10.4172/2157-7048.1000182>
- Ruan X, Li R, Ding Z et al (2019) Removal of Pb(II) Ions from aqueous solutions by spherical nanocomposites synthesized through immobilization of Paecilomyces lilacinus in silica nanoparticles coated with Ca-alginate. *J Nanosci Nanotechnol* 20:1907–1916. <https://doi.org/10.1166/jnn.2020.17349>
- Saber-Samandari S, Gazi M (2013) Cellulose-graft-polyacrylamide/hydroxyapatite composite hydrogel with possible application in removal of Cu (II) ions. *Elsevier Ltd Ltd* 73:1523–1530. <https://doi.org/10.1016/j.reactfunctpolym.2013.07.007>
- Santhosh C, Daneshvar E, Tripathi KM et al (2020) Synthesis and characterization of magnetic biochar adsorbents for the removal of Cr(VI) and acid orange 7 dye from aqueous solution. *Environ Sci Pollut Res*. <https://doi.org/10.1007/s11356-020-09275-1>
- Sattar MS, Shakoor MB, Ali S et al (2019) Comparative efficiency of peanut shell and peanut shell biochar for removal of arsenic from water. *Environ Sci Pollut Res* 26:18624–18635. <https://doi.org/10.1007/s11356-019-05185-z>
- Sewu DD, Boakye P, Jung H, Woo SH (2017) Synergistic dye adsorption by biochar from co-pyrolysis of spent mushroom substrate and *Saccharina japonica*. *Bioresour Technol* 244:1142–1149. <https://doi.org/10.1016/j.biortech.2017.08.103>
- Shackley S, Hammond J, Gaunt J, Ibarrola R (2011) The feasibility and costs of biochar deployment in the UK. *Carbon Manag* 2:335–356. <https://doi.org/10.4155/cmt.11.22>
- Shafiq M, Alazba AA, Amin MT (2019) Synthesis, characterization, and application of date palm leaf waste-derived biochar to remove cadmium and hazardous cationic dyes from synthetic wastewater. *Arab J Geosci*. <https://doi.org/10.1007/s12517-018-4186-y>
- Shanehsaz M, Seidi S, Ghorbani Y et al (2015) Polypyrrole-coated magnetic nanoparticles as an efficient adsorbent for RB19 synthetic textile dye: Removal and kinetic study. *Spectrochim Acta Part A Mol Biomol Spectrosc* 149:481–486. <https://doi.org/10.1016/j.saa.2015.04.114>
- Shao N, Li S, Yan F et al (2020) An all-in-one strategy for the adsorption of heavy metal ions and photodegradation of organic pollutants using steel slag-derived calcium silicate hydrate. *J Hazard Mater* 382:121120. <https://doi.org/10.1016/j.jhazmat.2019.121120>
- Sherlala AIA, Raman AAA, Bello MM, Asghar A (2018) A review of the applications of organo-functionalized magnetic graphene oxide nanocomposites for heavy metal adsorption. *Chemosphere* 193:1004–1017. <https://doi.org/10.1016/j.chemosphere.2017.11.093>
- Simsek EB, Beker U (2014) Equilibrium arsenic adsorption onto metallic oxides: Isotherm models, error analysis and removal mechanism. *Korean J Chem Eng* 31:2057–2069. <https://doi.org/10.1007/s11814-014-0176-2>
- Soares SF, Fernandes T, Trindade T, Daniel-da-Silva AL (2020) Recent advances on magnetic biosorbents and their applications for water treatment. *Environ Chem Lett* 18:151–164. <https://doi.org/10.1007/s10311-019-00931-8>
- Sun C, Huang Z, Wang J et al (2016) Modification of microcrystalline cellulose with pyridone derivatives for removal of cationic dyes from aqueous solutions. *Cellulose* 23:2917–2927. <https://doi.org/10.1007/s10570-016-1024-9>
- Sun, Ni J, Zhao C et al (2017) Preparation of a cellulosic adsorbent by functionalization with pyridone diacid for removal of Pb(II) and Co(II) from aqueous solutions. *Cellulose* 24:5615–5624. <https://doi.org/10.1007/s10570-017-1519-z>
- Tan CHC, Sabar S, Hussin MH (2018) Development of immobilized microcrystalline cellulose as an effective adsorbent for methylene blue dye removal. *South African J Chem Eng* 26:11–24. <https://doi.org/10.1016/j.sajce.2018.08.001>
- Tang Y, Ma Q, Luo Y et al (2013) Improved synthesis of a branched poly(ethylene imine)-modified cellulose-based adsorbent for removal and recovery of Cu(II) from aqueous solution. *J Appl Polym Sci* 129:1799–1805. <https://doi.org/10.1002/app.38878>
- Varghese AG, Paul SA, Latha MS (2019) Remediation of heavy metals and dyes from wastewater using cellulose-based adsorbents. *Environ Chem Lett* 17:867–877. <https://doi.org/10.1007/s10311-018-00843-z>
- Vicente-Martínez Y, Caravaca M, Soto-Meca A (2020) Total removal of Hg (II) from wastewater using magnetic nanoparticles coated with nanometric Ag and functionalized with sodium 2-mercaptoethane sulfonate. *Environ Chem Lett* 18:975–981. <https://doi.org/10.1007/s10311-020-00987-x>
- Vijayalakshmi K, Devi BM, Latha S et al (2017) Batch adsorption and desorption studies on the removal of lead (II) from aqueous solution using nanochitosan/sodium alginate/microcrystalline cellulose beads. *Int J Biol Macromol* 104:1483–1494. <https://doi.org/10.1016/j.ijbiomac.2017.04.120>
- Vimonses V, Lei S, Jin B et al (2009) Kinetic study and equilibrium isotherm analysis of congo red adsorption by clay materials. *Chem Eng J* 148:354–364. <https://doi.org/10.1016/j.cej.2008.09.009>
- Vishnu D, Dhandapani B (2020) Integration of *Cynodon dactylon* and *Muraya koenigii* plant extracts in amino-functionalised silica-coated magnetic nanoparticle as an effective sorbent for the removal of chromium(VI) metal pollutants. *IET Nanobiotechnol*. <https://doi.org/10.1049/iet-nbt.2019.0313>
- Vishnu D, Dhandapani B (2019) The symbiotic effect of integrated *Muraya koenigii* extract and surface-modified magnetic microspheres—a green biosorbent for the removal of Cu(II) and Cr(VI) ions from aqueous solutions. *Chem Eng Commun*. <https://doi.org/10.1080/00986445.2019.1691538>
- Vishnu D, Dhandapani B, Ramakrishnan SR et al (2020) Fabrication of surface-engineered superparamagnetic nanocomposites (Co/Fe/Mn) with biochar from groundnut waste residues for the elimination of copper and lead metal ions. *J Nanostructure Chem*. <https://doi.org/10.1007/s40097-020-00360-y>
- Vishnu D, Neeraj G, Swaroopini R et al (2017) Synergistic integration of laccase and versatile peroxidase with magnetic silica

- microspheres towards remediation of biorefinery wastewater. *Environ Sci Pollut Res* 24:17993–18009. <https://doi.org/10.1007/s11356-017-9318-5>
- Wan Ngah WS, Teong LC, Hanafiah MAKM (2011) Adsorption of dyes and heavy metal ions by chitosan composites: a review. *Carbohydr Polym* 83:1446–1456. <https://doi.org/10.1016/j.carbpol.2010.11.004>
- Wang C, Wang H (2018) Pb(II) sorption from aqueous solution by novel biochar loaded with nano-particles. *Chemosphere* 192:1–4. <https://doi.org/10.1016/j.chemosphere.2017.10.125>
- Wang J, Guo X (2020) Adsorption kinetic models: physical meanings, applications, and solving methods. *J Hazard Mater* 390:122156. <https://doi.org/10.1016/j.jhazmat.2020.122156>
- Wang S, Kwak J, Islam S et al (2020) Science of the Total Environment Biochar surface complexation and Ni (II), Cu (II), and Cd (II) adsorption in aqueous solutions depend on feedstock type. *Sci Total Environ* 712:136538. <https://doi.org/10.1016/j.scitotenv.2020.136538>
- Wang S, Peng Y (2010) Natural zeolites as effective adsorbents in water and wastewater treatment. *Chem Eng J* 156:11–24. <https://doi.org/10.1016/j.cej.2009.10.029>
- Wang Y, Liu R (2017) Comparison of characteristics of twenty-one types of biochar and their ability to remove multi-heavy metals and methylene blue in solution. *Fuel Process Technol* 160:55–63. <https://doi.org/10.1016/j.fuproc.2017.02.019>
- Wathukarage A, Herath I, Iqbal MCM, Vithanage M (2019) Mechanistic understanding of crystal violet dye sorption by woody biochar: implications for wastewater treatment. *Environ Geochem Health* 41:1647–1661. <https://doi.org/10.1007/s10653-017-0013-8>
- Wei X, Huang T, Nie J et al (2018) Bio-inspired functionalization of microcrystalline cellulose aerogel with high adsorption performance toward dyes. *Carbohydr Polym* 198:546–555. <https://doi.org/10.1016/j.carbpol.2018.06.112>
- Wei X, Huang T, Yang J et al (2017) Green synthesis of hybrid graphene oxide/microcrystalline cellulose aerogels and their use as superabsorbents. *J Hazard Mater* 335:28–38. <https://doi.org/10.1016/j.jhazmat.2017.04.030>
- Xiao F, Cheng J, Cao W et al (2019a) Removal of heavy metals from aqueous solution using chitosan-combined magnetic biochars. *J Colloid Interface Sci* 540:579–584. <https://doi.org/10.1016/j.jcis.2019.01.068>
- Xiao H, Li C, Wang P, Zhao T (2019b) A feasible approach for enhancing union dyeing of wool/acrylic blend fabrics with heterobifunctional cationic reactive dyes. *Text Res J* 89:5085–5095. <https://doi.org/10.1177/0040517519849452>
- Xin X, Wei Q, Yang J et al (2012) Highly efficient removal of heavy metal ions by amine-functionalized mesoporous Fe₃O₄ nanoparticles. *Chem Eng J* 184:132–140. <https://doi.org/10.1016/j.cej.2012.01.016>
- Xue yan X, Cheng R, Shi L et al (2017) Nanomaterials for water pollution monitoring and remediation. *Environ Chem Lett* 15:23–27. <https://doi.org/10.1007/s10311-016-0595-x>
- Yan L, Kong L, Qu Z et al (2015) Magnetic biochar decorated with ZnS nanocrystals for Pb (II) removal. *ACS Sustain Chem Eng* 3:125–132. <https://doi.org/10.1021/sc500619r>
- Yavari S, Mahmodi NM, Teymouri P et al (2016) Cobalt ferrite nanoparticles: Preparation, characterization and anionic dye removal capability. *J Taiwan Inst Chem Eng* 59:320–329. <https://doi.org/10.1016/j.jtice.2015.08.011>
- Yi Y, Huang Z, Lu B et al (2019) Magnetic biochar for environmental remediation: A review. *Bioresour Technol*. <https://doi.org/10.1016/j.biortech.2019.122468>
- Yu Z, Hu C, Dichiaro AB et al (2020) Cellulose nanofibril/carbon nanomaterial hybrid aerogels for adsorption removal of cationic and anionic organic dyes. *Nanomaterials* 10:1–20. <https://doi.org/10.3390/nano10010169>
- Zaman A, Orasugh JT, Banerjee P et al (2020) Facile one-pot in-situ synthesis of novel graphene oxide-cellulose nanocomposite for enhanced azo dye adsorption at optimized conditions. *Carbohydr Polym* 246:116661. <https://doi.org/10.1016/j.carbpol.2020.116661>
- Zango ZU, Shehu Imam S (2018) Evaluation of microcrystalline cellulose from groundnut shell for the removal of crystal violet and methylene blue. *Nanosci Nanotechnol* 8:1–6. <https://doi.org/10.5923/j.nn.20180801.01>
- Zhou Y, Lu J, Zhou Y, Liu Y (2019) Recent advances for dyes removal using novel adsorbents: a review. *Environ Pollut* 252:352–365. <https://doi.org/10.1016/j.envpol.2019.05.072>
- Zhu Y, Liang H, Yu R et al (2020) Removal of aquatic cadmium ions using thiourea modified poplar biochar. *Water (Switzerland)*. <https://doi.org/10.3390/W12041117>

Publisher's Note Springer Nature remains neutral with regard to jurisdictional claims in published maps and institutional affiliations.